1 **Effect of oxidation and *in vitro* intestinal hydrolysis on phospholipid toxicity towards**

2 **HT29 cell line serving as a model of human intestinal epithelium**

3

4 Karol Parchem[a]*, Monika Baranowska[a], Anna Kościelak[a], Ilona Kłosowska-Chomiczewska[b], Maria

5 Rosário Domingues[c,d], Adam Macierzanka[b], Agnieszka Bartoszek[a]

6

7 [a] Department of Food Chemistry, Technology and Biotechnology, Faculty of Chemistry, Gdańsk

8 University of Technology, 11/12 Gabriela Narutowicza St., 80-233 Gdansk, Poland,

9 karol.parchem@pg.edu.pl or parchem.karol@gmail.com (K.P.) bbmmonik@gmail.com (M.B.)

10 anna.koscielak@pg.edu.pl (A.K.), agnieszka.bartoszek@pg.edu.pl (A.B.)

11

12 [b] Department of Colloid and Lipid Science, Faculty of Chemistry, Gdańsk University of Technology,

13 11/12 Gabriela Narutowicza St., 80-233 Gdansk, Poland, ilona.chomiczewska@pg.edu.pl (I.K-C),

14 adam.macierzanka@pg.edu.pl (A.M.)

15

16 [c] Mass Spectrometry Centre, LAQV-REQUIMTE, Department of Chemistry, University of Aveiro,

17 Santiago University Campus, 3810-193 Aveiro, Portugal, mrd@ua.pt (M.R.D)

18

19 [d] Centre for Environmental and Marine Studies, CESAM, Department of Chemistry, University of

20 Aveiro, Santiago University Campus, 3810-193 Aveiro, Portugal, mrd@ua.pt (M.R.D)

21

22 *Corresponding author:

23 *E-mail address*: karol.parchem@pg.edu.pl or parchem.karol@gmail.com (K. Parchem)

24

25 Declarations of interest: none

26 Color figures only in the *online* version

Abstract

Oxidation of food-derived phospholipids (PLs) can influence nutrient digestion and induce oxidative stress in gastrointestinal epithelium. In this study, hen egg yolk PL fraction was used to evaluate the effect of lipoxygenase (LOX)-induced PL oxidation on the hydrolysis of PLs catalyzed by pancreatic phospholipase A_2 (PLA_2) in the presence of bile salts (BSs). Then, PL/BS solutions containing native or oxidized PLs were used in *in vitro* intestinal digestion to assess the effect of PL oxidation and hydrolysis on the toxicity towards HT29 cell line. Based on the obtained results, we suggest that hexanal and (*E*)-2-nonenal, formed by the decomposition of PL hydroperoxides, inhibited PLA_2 activity. The cell exposure to simulated intestinal fluid (SIF) containing BSs decreased HT29 cell viability and significantly damaged cellular DNA. However, the genotoxic effect was reversed in the presence of all tested PL samples, while the protective effect against the BS-induced cytotoxicity was observed for native non-hydrolyzed PLs, but was not clearly visible for other samples. This can result from an overlap of other toxic effects such as lipotoxicity or disturbance of cellular redox homeostasis. Tacking into account the data obtained, it was proposed that the PLA_2 activity decline in the presence of PL oxidation products may be a kind of protective mechanism against rapid release of oxidized FAs characterized by high cytotoxic effect towards intestinal epithelium cells.

Key words: oxidized phospholipids; phospholipid hydrolysis; pancreatic phospholipase A_2; bile salts; intestinal oxidative stress;

Abbreviations: BS – bile salts; CLD – cytosolic lipid droplets; ER – endoplasmic reticulum; FA – fatty acid; FAME – fatty acid methyl ester; GPx2 – gastrointestinal glutathione peroxidase 2; GSH – glutathione; GSSG – glutathione disulfide; IC – inhibitory concentration IEC – intestine epithelial cell; LOH – lipid hydroxide; LOOH – lipid hydroperoxide; LOP – lipid oxidation products; LOX – lipoxygenase; LPL – lysophospholipid; MDA – malondialdehyde; O/W – oil-in water emulsion; oxPL – oxidized phospholipid; PC – phosphatidylcholine; PDI – polydispersity index; PE – phosphatidylethanolamine; PL – phospholipid; PLA_2 – phospholipase A_2; PUFA – polyunsaturated fatty acid; PV – peroxide value; RNS – reactive nitrogen species; ROS – reactive oxygen species; SFA – saturated fatty acid; SIF – simulated intestinal fluid; TAG – triacylglycerol; TBARS – thiobarbituric acid reactive substances; UFA – unsaturated fatty acid.

1. Introduction

Phospholipids (PLs) are important biomolecules, which apart from building cell and organelle membranes, also play a role of endogenous signalling molecules. The biophysical properties of membranes, including their fluidity and permeability as well as the distribution and activity of embedded proteins, are related to the composition of lipid bilayer, including PL structures or cholesterol to PL ratio (Küllenberg de Gaudry, Taylor, Schneider, & Massing, 2012). Moreover, polyunsaturated fatty acids (PUFAs) present in the structure of membrane PLs can be oxidatively modified under oxidative stress conditions. Such modifications change hydrophobicity of the fatty acids (FAs) build in the PL structure, which perturbs the assembly of the cellular membranes and alters their functional properties, e.g., by disturbing ion and nutrient transport (Catalá, 2012; Catalá & Díaz, 2016). Additionally, endogenous oxidized PLs (oxPLs) may be recognized by specific receptors leading to the activation of signaling pathways that mediate the inflammatory response or cell apoptosis (Fruhwirth, Loidl, & Hermetter, 2007). Therefore, elevated levels of cellular or plasma oxPLs are believed to be implicated in the pathogeneses of some diseases and disorders (Parchem, Sasson, Ferreri, & Bartoszek, 2019). The endogenous abundance of oxPLs increases i.a., under the conditions of cellular oxidative stress, which results from imbalance between the prooxidant and antioxidant systems, and consequently the excessive production of reactive oxygen and nitrogen species (ROS/RNS).

Diet is one of the most relevant factors that can modulate cellular and tissue levels of ROS/RNS. It has been demonstrated that an overload of nutrients, especially caused by high-fat or/and high-glucose diets can be implicated in the disruption of cellular redox homeostasis. One of the mechanisms involved in oxidative stress induced by high-energy-dense diets is lipotoxicity, which result from inadequate lipid storage capacity in adipose tissue and/or abnormal adipose tissue lipolysis (Montgomery, De Nardo, & Watt, 2019). This leads to chronically elevated levels of plasma non-esterified FAs and increased ectopic lipid deposition. As a consequence, lipotoxic cellular outcomes including endoplasmic reticulum (ER) stress, inflammation, mitochondrial dysfunction and finally cell apoptosis can occur (Montgomery et al., 2019). Diet-related oxidative stress may result in dysfunction of various gastrointestinal cell types such as hepatocytes (Lian, Zhai, Li, & Wang, 2020), pancreatic β-cells (Sasson, 2017) or intestine epithelial cells (IECs) (Gulhane et al., 2016). The latter can be exposed to overhigh FA concentration in both, basolateral and apical sides (Bashllari et al., 2020; Van

3

88   Rijn et al., 2019). Another factor that can trigger cellular oxidative stress is an exposition of IECs to

89   food-delivered lipid oxidation products (LOPs) (Awada et al., 2012). PUFAs present in the structure of

90   dietary lipids are highly prone to oxidative modifications during food processing and storage

91   (Wąsowicz et al., 2004) as well as in the gastrointestinal digestion (Nieva-Echevarría, Goicoechea, &

92   Guillén, 2018). Importantly, previous studies indicated that for foods such as fish or meat, oxidative

93   changes first occurred in PLs and then in triacylglycerols (TAGs) (Igene, Pearson, Dugan, & Price,

94   1980; Jittrepotch, Ushio, & Ohshima, 2006). This order result from higher unsaturation of FAs in the

95   structures of muscle PLs compare to TAGs from the same origin (Cui & Decker, 2016; Guyon,

96   Meynier, & de Lamballerie, 2016). Additionally, it seams that PLs, due to their presence in cellular

97   membranes characterized by large surface area, are more exposed to prooxidant molecules (Cui &

98   Decker, 2016).

99   PLs, next to bile salts (BS), are surface-active compounds that facilitate solubilization of ingested oils

100   and fats, leading to the formation of an oil-in water (O/W) emulsion. As a result of pancreatic lipolytic

101   enzyme activity, dietary lipids are hydrolyzed, and the formed products are removed form the O/W

102   surface. However, the presence of oxidized (phospho)lipids in the colloidal structures subjected to

103   intestinal digestion can change the kinetics of lipolysis. So far, this topic has only been covered in few

104   research studies. For example, Baba et al., observed that porcine pancreatic PLA$_2$ preferentially

105   released 13(S)-hydroperoxy-(9Z,11E)-octadecadienoic acid from the *sn*-2 position of

106   phosphatidylcholine (PC) molecule in the presence of sodium deoxycholate compared to non-oxidized

107   PC species (Baba, Mikami, Shigeta, Nakajima, & Matsuo, 1993). In another study, the authors

108   monitored the activity of porcine pancreatic PLA$_2$ towards UV-irradiated hen egg yolk PC species in

109   PC/sodium deoxycholate mixed micelle structures compared to the non-irradiated sample (Litvinko,

110   Skorostetskaya, & Gerlovsky, 2018). The obtained data revealed the increase in the rate of PLA$_2$-

111   catalyzed hydrolysis of PC fraction exposed up to 40 min to the UV-irradiation, while after this time the

112   enzymatic activity declined. It was suggested that the presence of primary product of PC oxidation (PC

113   hydroperoxides) lead to PLA$_2$ activation and efficient removal of oxidatively modified FA from the PC

114   structure. After 40 min of PC irradiation, a significant increase in malondialdehyde (MDA) level was

115   observed. Probably, MDA and other highly reactive secondary lipid oxidation products were

116   responsible for the inhibition of PLA$_2$ activity (Litvinko et al., 2018).

117   As mentioned earlier, increased absorption and accumulation of oxidized lipids and products of their

4

118 decomposition, such as 4-hydroxy-2-alkenals, by IECs can contribute to the disruption of cellular

119 redox homeostasis. However, exposure of human colon adenocarcinoma Caco-2/TC7 cells to a

120 relatively low LOP concentration has been shown to induce cellular antioxidant systems including

121 overexpression of gastrointestinal glutathione peroxidase 2 (GPx2) (Awada et al., 2012). This enzyme

122 is responsible for detoxification and degradation of hydrogen peroxide (H_2O_2) and lipid hydroperoxides

123 (LOOHs) to water and lipid hydroxides (LOH), respectively (Awada et al., 2012). Elevated LOP

124 concentration and/or chronic cell exposure to these products can disrupt cellular antioxidant systems.

125 The previous *in vivo* study in rats indicated that chronic exposure to subtoxic level of oxidized fish oil

126 led to a decrease in the intestinal tissue glutathione (GSH) in favour of glutathione disulfide (GSSG)

127 concentration (Tsunada et al., 2003). Moreover, the disturbance of intestinal GSH/GSSG ratio

128 resulting from cell exposure to oxidized lipids, induced cellular transitions from proliferation to growth

129 arrest and apoptosis (Tsunada et al., 2003). This example clearly indicated the effects of redox

130 imbalance on intestinal cell dysfunction.

131 The main cellular structures that can by modified due to oxidative stress include membrane lipids,

132 proteins and nucleic acids. Concerning ROS-induced modifications of (phospho)lipids, these include

133 hydroxylation, peroxidation or carbonylation of unsaturated FAs (UFAs) as well as the cleavage of the

134 C-C bond along FA acyl chain to form truncated (phospho)lipids (T. Y. Wang, Libardo, Angeles-Boza,

135 & Pellois, 2017). Such oxidative alterations of UFAs present within membrane PLs prevent their

136 immersion in the interior of the bilayer and lead to the translocation of oxidized FAs onto membrane

137 surface in the form of so-called "whiskers" (Catalá, 2015). The accumulation of such aberrant

138 structures can alter plasma, mitochondrial or ER membrane properties and thus their functions.

139 Therefore, the modified membranes require reconstruction to maintain their original biophysical and

140 functional properties. Oxidatively modified acyl chains of membrane PLs can be removed from the

141 backbone upon hydrolysis catalyzed by intracellular or plasma phospholipases A_2 (PLA$_2$) (Fruhwirth et

142 al., 2007), followed by re-acylation of membrane PLs to restore their original structure. It has been

143 suggested that the dynamic pool of undamaged UFAs for the membrane PL re-synthesis is provided

144 by cellular TAGs stored in cytosolic lipid droplets (CLDs) (Girón-Calle, Schmid, & Schmid, 1997;

145 Pamplona, 2008). The accumulation and FA composition of TAGs in CLDs strictly depend on the

146 amount and the type of ingested lipids, especially in the case of IECs. The products of the intestinal

147 lipolysis are re-synthesized to TAGs or PLs at the ER membrane after their absorption by enterocytes.

5

148 Next, in the ER lumen, the formed lipids are used for assembling of chylomicrons, which are finally

149 secreted *via* lymphatic system to bloodstream (Beilstein, Carrière, Leturque, & Demignot, 2016). In

150 order to avoid postprandial hypertriglyceridemia, the re-synthesized lipids may be temporary stored in

151 the CLDs of enterocytes. In this period, enterocytes can hydrolyze esterified lipids and use the

152 released FAs for their own needs e.g., energy production or membrane biosynthesis. In the

153 interprandial phase, the storage lipids can be mobilized for chylomicron formation (Beilstein et al.,

154 2016).

155 Another way of repairing damaged cellular membranes implies a direct incorporation of orally

156 administrated PLs into cellular lipid bilayers. Such an approach, called lipid replacement therapy was

157 proposed by Nicolson and involves a delivery of PLs to tissues and cells with limitations of their

158 oxidation during the storage, ingestion, digestion and uptake as well as prevention of the intestinal

159 hydrolysis of orally-administered PLs (Nicolson & Ash, 2014). Interestingly, some literature data

160 indicated that even 20 % of dietary PLs can be absorbed by enterocytes in undigested form

161 (Küllenberg de Gaudry et al., 2012) and potentially directly affect the membrane lipid remodelling.

162 However, most of the consumed PLs are hydrolyzed in the small intestine by pancreatic

163 phospholipase A_2 (PLA_2) to lysophospholipids (LPLs) and FAs and then re-synthesized at the ER

164 membrane.

165 Food-delivered PLs are known for their high nutritional value and beneficial health effects, not only as

166 a source of essential FAs, but also due to their anti-inflammatory, antioxidant, antifibrogenic,

167 membrane-protective and lipid-regulating properties (Blesso, 2015; Gundermann, Gundermann,

168 Drozdzik, & Mohan Prasad, 2016; Küllenberg de Gaudry et al., 2012). However, PLs, especially those

169 rich in PUFAs, are susceptible to oxidative modifications during the food processing and storage as

170 well as the gastrointestinal digestion. Nevertheless, to date, data on the influence of PL oxidation on

171 their intestinal digestion and the biological effect of the resulting products on IECs are limited.

172 Therefore, in our study, we proposed several research models to understand step-by-step the role of

173 PL oxidation and intestinal hydrolysis on IEC physiology and pathophysiology. The aim of this study

174 was threefold: (i) to evaluate the effect of lipoxygenase (LOX)-induced oxidative modification of egg

175 yolk PL fraction on the parameters of colloidal structure found in the simulated *in vitro* intestinal fluid

176 containing bile salts (BSs); (ii) to determine the effect of PL oxidation on the kinetics of their *in vitro*

177 intestinal hydrolysis catalyzed by pancreatic PLA_2 in the presence of BSs, and (iii) to assess the

6

178 impact of native and oxidized PLs, both before and after *in vitro* intestinal hydrolysis, on HT29 cell

179 physiology, serving as a model of intestinal tissue exposed to direct contact with ingested food

180 ingredients. This cell line is a human intestinal epithelial cell line derived from human colorectal

181 adenocarcinoma. However, HT29 cells express features of both absorptive enterocytes and intestinal

182 secretory cells producing a gelatinous mucus-like substance (Fedi et al., 2021). Additionally, its

183 differentiated phenotype is similar to small intestine enterocytes in terms of their structure and the

184 presence of brush border-associated hydrolases (Martínez-Maqueda, Miralles, & Recio, 2015).

185 Therefore, this cell line has been widely used in *in vitro* studies of cellular absorption, bioavailability

186 and metabolism of food molecules (Martínez-Maqueda et al., 2015). Nevertheless, it should be noted

187 that this cellular model has some disadvantage arising from cancerous and non-small intestinal origin,

188 therefore differences in the gene expression of transporters and metabolic enzymes can be observed

189 compare to the normal small intestinal cells (Fedi et al., 2021; Martínez-Maqueda et al., 2015).

190 However, the aim of this research was to evaluate the effect of PL oxidation and hydrolysis on

191 physiology of IECs and understanding the mechanism of toxicity of formed products, therefore we

192 found this model to be appropriate.

193 **2. Materials and methods**

194 **2.1. Chemicals and materials**

195 Acetic acid, acetone, chloroform, hexane, methanol, ethanol (96 %), boric acid, disodium tetraborate

196 decahydrate, sulphuric acid, hydrochloric acid (HCl), potassium iodine, sodium thiosulfate, sodium

197 chloride (NaCl), calcium chloride (CaCl$_2$), 2-amino-2-(hydroxymethyl)-1,3-propanediol (Tris-base), 0.1

198 M sodium hydroxide solution (NaOH), ethylenediaminetetraacetic acid (EDTA) (all ACS grade) and

199 acetonitrile (HPLC gradient grade) were purchased from Merck KGaA (Darmstadt, Germany).

200 Ammonium formate (LC-MS grade) was obtained from VWR International (Leicestershire, UK).

201 Lipoxidase from *Glycine max* (soybean) type I-B (LOX-1), sodium deoxycholate (≥98%), molybdenum

202 (≥99.9), molybdenum (VI) oxide (≥99.9), fatty acid methyl ester (FAME) standards, trichloroacetic acid

203 (TCA), thiobarbituric acid (TBA), butylated hydroxytoluene (BHT), olive oil highly refined, bile salt (BS)

204 mixture (United States Pharmacopeia Reference Standard), pancreatic phospholipase A$_2$ (PLA$_2$),

205 Varespladib (≥98%), thiazolyl blue tetrazolium bromide (MTT), dimethyl sulfoxide (DMSO), tablets of

206 phosphate buffered saline (PBS), low melting point agarose (LMP agarose), Sybr Green I nucleic acid

207 gel stain, Triton X100, formaldehyde, Nile Red were derived from Sigma-Aldrich, Merck KGaA

208 (Darmstadt, Germany). Normal melting point agarose (NMP agarose) was obtained form Bioline

209 (London, United Kingdom). High purity water was produced using Millipore Elix 5 purification system

210 (Darmstadt, Germany). Fresh free-range hen eggs with a mass in the range of 63-73 g were

211 purchased in a local market (Gdansk, Poland).

212 **2.2. Study design**

213 PL fraction was isolated from fresh hen eggs and its composition was characterized by

214 chromatography taking into account PL classes and FA composition (Fig. 1). In order to determine the

215 effect of oxidative modification of PL on the kinetics of their hydrolysis and potential toxicity towards

216 intestinal cells, part of the native PL fraction was enzymatically oxidized by LOX. The degree of PL

217 oxidation was assessed by determination of peroxide value (PV) and thiobarbituric acid reactive

218 substances (TBARS). In the next step, native and oxidized PLs were used to prepare aggregation

219 structures (mixed micelles solutions and emulsions) in simulated intestinal fluid (SIF) containing BS

220 whose concentration matched physiological levels. The BS concentration in the prepared solutions

221 was calculated based the average molecular mass of commercially available BS mixture (c.a. 519.0

222 g/mol) and was about 9.6 mM. While the physiological BS concentration in the postprandial state

223 range from 4 – 20 mM (Maldonado-Valderrama, Wilde, MacIerzanka, & MacKie, 2011). The obtained

224 aggregation structures were characterized in terms of size distribution and dispersity and then

225 subjected to *in vitro* intestinal digestion. The kinetics of PL hydrolysis catalyzed by porcine pancreatic

226 PLA_2 was monitored using pH-stat titration (pH=8). The samples of native and oxidized PL/BS mixed

227 micelle solutions before and after hydrolysis were then used for comparisons of their biological effects.

228 One of the cell lines recommended by the Replacement, Refinement and Reduction of Animals in

229 Research for nutritional studies is HT29 (human colon adenocarcinoma) cell line, which was employed

230 in this study (Krishna & Gopalakrishnan, 2016). The PL/BS mixed micelle solutions were added to cell

231 culture medium in the amount of 10 % *v/v*. The impact of PL oxidation and hydrolysis on cell

232 physiology was evaluated by determination of cell viability by MTT test, genotoxicity by comet assay

233 and ability of cells to neutral lipid accumulation using fluorescence microscopy.

8
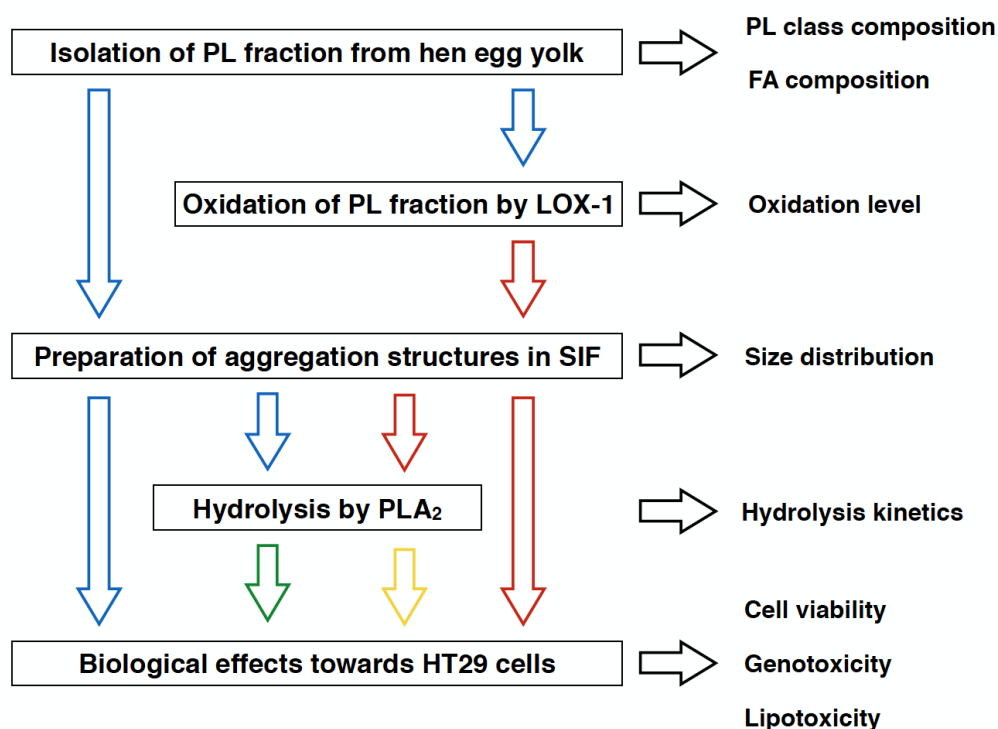
Fig. 1. Study design. (Abbreviations: FA – fatty acid; LOX-1 – lipoxygenase type 1; PL – phospholipid; PLA$_2$ – phospholipase A$_2$; SIF – simulated intestinal fluid)

2.3. Isolation of hen egg yolk PL fraction

Hen egg yolk PL fraction was isolated as described previously by Gładkowski et al. (Gładkowski, Chojnacka, Kiełbowicz, Trziszka, & Wawrzeńczyk, 2012) with further modifications (Parchem, Kusznierewicz, Chmiel, Maciołek, & Bartoszek, 2019). Briefly, two egg yolks were combined with 120 mL of methanol, stirred for 10 min and left at room temperature until the alcohol-insoluble fraction precipitated. Then, the supernatant was filtered and the precipitate was re-extracted twice with 120 mL of methanol. The extracts were combined and the solvent was evaporated under reduced pressure at 40 °C using a rotary evaporator. The residue was dissolved in 20 mL of hexane and transferred to a glass flask placed in an ice bath. Afterwards, under constant stirring, 120 mL of cold acetone at −20 °C was carefully added until PL fraction precipitated. The precipitate was then carefully washed 3 times with 40 mL of cold acetone at −20 °C and the solvent was removed each time by decantation. Finally, the PL fraction was dried in a stream of nitrogen, frozen overnight at −20 °C and freeze-dried for 48 h using laboratory freeze dryer Alpha 1-4 (Christ, Germany). The samples were stored at −80 °C in nitrogen atmosphere until used for experiments.

2.4. Lipoxygenase-catalyzed oxidation of egg yolk PLs

252   The enzymatic peroxidation was carried out as described previously by Butler O'Connor et al. (Butler

253   O'Connor et al., 2010) with further modifications (Parchem, Kusznierewicz, et al., 2019). The

254   methanolic solution of egg yolk PL fraction (20 mg/mL) was perpetrated in a round bottom flask.

255   Methanol was evaporated under reduced pressure at 40 °C using a rotary evaporator and the PL

256   fraction was dried at room temperature for 1 h in a stream of nitrogen. The obtained PL film was then

257   hydrated with borate buffer (0.2 M, pH=9) containing 10 mM sodium deoxycholate. Prior to the

258   addition of bile salt, the buffer was saturated with oxygen at room temperature for 30 min. Enzymatic

259   peroxidation of PL was initiated by adding freshly prepared soybean lipoxidase type 1 (LOX-1) solution

260   in the borate buffer. The final PL concentration was 5 mg/mL and the LOX-1 activity was 70 kU/mL.

261   The reaction was carried out at 37 °C under oxygen atmosphere for 1 h. The peroxidation was

262   stopped by the addition of chloroform/methanol mixture (2:1 *v/v*) in a volume equal to the volume of

263   the reaction mixture. After intense shaking, the mixture was distributed to glass tubes and centrifuged

264   (1600 × *g*, 5 min). The upper organic layer was transferred with a glass Pasteur pipettes to a round

265   bottom flask. Then, the solvent was evaporated under a stream of nitrogen at 40 °C, frozen overnight

266   at −20 °C, followed by freeze-drying for 48 h using laboratory freeze dryer Alpha 1-4 (Christ,

267   Germany). The samples were stored at −80 °C in nitrogen atmosphere for further experiments.

268   **2.5. Characterization of egg yolk PL fraction**

269   **2.5.1. Chromatographic analysis of PL classes**

270   Hen egg yolk PL classes were analyzed using hydrophilic interaction liquid chromatography (HILIC) as

271   described previously by Lisa et al. (Lísa, Cífková, & Holčapek, 2011) with further modifications

272   (Parchem, Kusznierewicz, et al., 2019). The separation of individual PL classes was performed using

273   a Dionex UltiMate 3000 LC system (Thermo Scientific, USA) equipped with a Rx-SIL column (250 ×

274   4.5 mm, 5 μm) (Agilent Technology, USA). The mobile phase consisted of acetonitrile (A) and 5 mM

275   aqueous ammonium formate (B). The gradient program was as follows: 0 – 30 min, 6 – 77 % B, 30 –

276   35 min, 77 % B, finally the column was re-equilibrated to the initial conditions for 20 min. The

277   separation was carried out at of 40 °C with a flow rate of 1 mL/min. The injection volume was 20 μL.

278   The eluted PL classes were monitored using a Corona Ultra RS CAD (Thermo Scientific, USA) with

279   following parameters: acquisition range of 100 pA, digital filter set to "none", gas flow (air) of 12 L/min

280   and nebulizer pressure of 35 psi. Individual PL classes were identified by comparison of their retention

281   times with those of standards (more details: (Parchem, Kusznierewicz, et al., 2019)). Results are

282   expressed as a mean of three independent determinations of the percentage of the individual PL

283   classes in total PLs identified in the sample.

2.5.2. Analysis of FA composition in the structure of PC and PE fractions

285   The methanolic solution of PLs (20 mg/mL) in a volume of 100 µL was applied onto a preparative TLC

286   glass silica gel plate (20 × 20 cm, 1 mm, 10-12 µm) (Merck, Germany) as a 20 cm band using a hand-

287   held applicator equipped with a 100 µL syringe. PL classes were separated with

288   chloroform/methanol/acetic acid/water mixture (35:25:4:14:2 v/v/v/v) (Palusinska-Szysz, Kania,

289   Turska-Szewczuk, & Danikiewicz, 2014). After separation, the plate was dried using a stream of

290   nitrogen and sprayed with a molybdenum reagent (Dittmer & Lester, 1964) over a width of 2 cm in

291   order to locate individual PL classes. Then, silica gel from areas corresponding to the two main PL

292   classes present in egg yolk (PCs and phosphatidylethanolamines (Pes)) was scraped off from the

293   non-sprayed part of the plate using metal spatula. PC and PE fractions were extracted from the

294   appropriate portions of silica gel using 10 mL of chloroform/methanol (2:1 *v/v*) mixture. The extraction

295   was repeated twice. The obtained extracts corresponding to individual PL classes were combined and

296   the solvent was evaporated under reduced pressure at 40 °C using rotary evaporator.

297   Fas present in the structure of PCs and Pes were esterified to fatty acid methyl esters (FAMEs)

298   according to the European Standard [EN:ISO 5509:2000]. FAMEs were analyzed using high-

299   performance gas chromatography (HP-GC). The separation of FAMEs was performed using Perkin

300   Elmer Autosystem XL gas chromatograph (Perkin Elmer, USA) equipped with split injector 60:1 and

301   CP-Sil 88 column (50 m × 0,25 mm × 0,2 µm, Agilent Technology, USA). FAMEs were detected using

302   flame ionization detector (FID). The injector and FID temperatures were maintained at 250 °C. The

303   initial column temperature was 170 °C and held for 30 min, followed by an increase of 10 °C/min up to

304   200 °C and held for 15 min. Finally, the temperature was raised to 210 °C at a rate of 5 °C/min and

305   held for 10 min. Qualitative and quantitative analyses of Fas in the samples were performed using

306   FAME standards. Results are expressed as means of three independent determinations of the

307   percentage of the individual Fas in total Fas identified in the sample.

2.5.3. Determination of peroxide value of PL fraction

309   The peroxide value (PV) of native and oxidized PL fractions was determined according to the method

310   described previously (Fruehwirth et al., 2020) with some modifications. The appropriate amount of PL

11

311 fraction (1 g and 50 mg for native and oxidized PL fraction, respectively) was dissolved in 5 mL of

312 acetic acid/chloroform (3:2 *v/v*) mixture. The differences in weighted amounts between the native and

313 oxidized samples resulted from a significant difference in the content of PL hydroperoxides. Therefore,

314 the sample amount was optimized such that the volume of titrant added was between 2 and 18 mL

315 using a 20 mL burette. Then, 200 µL of a saturated potassium iodide solution was added, the sample

316 was shaken for 1 min and placed in darkness for 5 min. Afterwards, 15 mL of distilled water and few

317 droplets of 1 % *w/w* starch solution were added. The samples were titrated using 0.002 N sodium

318 thiosulfate solution until complete discoloration was reached. The blank test was performed without PL

319 fraction. The samples were analyzed in triplicate.

320 2.5.4. Determination of TBARS content

321 The amount of thiobarbituric acid reactive substances (TBARS) in native and oxidized PL fraction was

322 determined by method described by Fenaille et al. (Fenaille, Mottier, Turesky, Ali, & Guy, 2001) with

323 modifications. In brief, 1 mL of aqueous solutions of PL fraction (10 and 2.5 mg/mL for native and

324 oxidized PL fraction, respectively) was combined with 1 mL of reaction mixture containing equal

325 volumes of 15 % trichloroacetic acid (TCA), 0.25 M HCl and 0.375 % thiobarbituric acid (TBA),

326 followed by the addition of 0.1 mL of 0.4% solution of butylated hydroxytoluene (BHT) in 96% ethanol.

327 The differences in weighted amounts between the native and oxidized samples resulted from a

328 significant difference in the content TBARS. Therefore, the sample amount was optimized such that

329 the absorbance was below 1.5 as recommended by manufacturer. The sample was shaken for 1 min

330 and then centrifuged (4700 × *g*, 5 min). The supernatant was collected to the new tube, while the

331 precipitate was mixed with another 1 mL of reaction mixture, shaken and centrifuged. The combined

332 supernatants were incubated at 95 °C under nitrogen atmosphere for 30 min. Then, the reaction was

333 stopped by cooing the sample in an ice bath. The mixture was made up to 12 mL with distilled water

334 and centrifuged (4700 × *g*, 5 min). The absorbance of the supernatant was measured at wavelengths

335 of 532 and 600 nm as a background. The TBARS content was calculated based on molar extinction

336 coefficient (ε) for MDA-TBA$_2$ adduct (1.55×10^5 M^{-1} × cm^{-1}) (Meca et al., 2021). The samples were

337 analyzed in triplicate.

338 2.6. Preparation and characterization of PL/BS mixed micelles and PL/BS/TAG emulsions

12

339 The PL/BS mixed micelle solution was prepared by dispersing 1 % *w/v* egg yolk PL fractions in the

340 simulated intestinal fluid (SIF) containing 150 mM NaCl, 6 mM CaCl$_2$, 0.28 mM Tris-base and 5 mg/mL

341 of BS mixture. The composition of used BS mixture is shown in Supplementary Materials (Table A1).

342 The solution was then sonicated on ice (20 kHz, 4 min) to reduce the particle size and to homogenize

343 the mixed micelles using Vibra-Cell VC 750 ultrasound sources fitted with a 3 mm diameter titanium

344 micro-tip VCX500 (Sonics, USA). Power delivery was controlled as amplitude percentage, which was

345 set as 40 %. A pulsed duty cycle of 8 sec on and 2 sec off was used for all experiments. The

346 PL/BS/TAG emulsion was prepared by dispersing 1 % *w/v* egg yolk PL fractions and 1.5 % *w/v* highly

347 refined olive oil in SIF. The solution was then sonicated using the conditions outlined above.

348 The mixed micelle and emulsion droplet size distribution and dispersity (polydispersity index, PDI)

349 were determined using a non-invasive black scatter (NIBS) technique (Kupper, Kłosowska-

350 Chomiczewska, & Szumała, 2017). For this purpose, a Zetasizer Nano ZS (Malvern, United Kingdom)

351 equipped with a helium-neon laser diffraction operating at 633 nm was employed. For the mixed

352 micelles, the samples were analyzed directly without dilution, while the emulsion samples were diluted

353 with the buffer (150 mM NaCl, 6 mM CaCl$_2$, 0.28 mM Tris base, pH=8) in a ratio of 1:1000. All

354 measurements were performed at 37 °C. The samples were analyzed in quintuplicate.

355 **2.7. *In vitro* intestinal PL hydrolysis**

356 Four digestive systems, consisting of native or oxidized PL fraction without or with TAGs, have been

357 proposed to understand the effect of PL oxidation and the aggregation structure in which PL are

358 embedded on kinetics of their hydrolysis catalyzed by PLA$_2$. The kinetics of PL hydrolysis was

359 monitored using a pH-stat method, in which enzymatically released Fas were continually titrated with

360 0.1 M NaOH to keep the pH constant at 8.0. The mixed micelle solution or emulsion in the volume of

361 15 mL was placed in a titration vessel of the T70 titrator (Mettler Toledo, USA). The sample was pre-

362 incubated at 37 °C for 15 min until the temperature equilibration and then pH value was adjusted to

363 8.0 using 0.1 M NaOH and 0.1 M HCl. The reaction was initiated by the addition of porcine pancreatic

364 phospholipase A$_2$ (PLA$_2$) to reach the final activity of 35 U/mL. The PL hydrolysis was carried out at 37

365 °C with continuous stirring (40 % of the maximum stirring speed). Unless otherwise stated, the

366 hydrolysis reaction was carried out for 1 h. Hydrolysis reactions were carried out in triplicate for each

367 sample type.

2.8. PLA$_2$ activity in the presence of aldehydes

The native PL/BS mixed micelles solution was prepared as described in section 2.6. The samples was placed in the titration vessel of the T70 titrator (Mettler Toledo, USA) and pre-incubated at 37 °C for 15 min. Then, appropriate volumes of low-molecular aldehydes (hexanal or €-2-nonenal), corresponding to the following final concentrations: 0, 5, 10, 15, 20 mM, were added. For this range, a negative linear correlation was observed between the concentration of tested aldehydes and the PLA$_2$ activity, which allowed for determination of IC$_{10}$ and IC$_{30}$ values. The pH value was adjusted to 8.0 followed by addition of porcine pancreatic PLA$_2$) with the final activity of 30 U/mL. PLA$_2$ activity was calculated based on the volume of 0.1 M NaOH added after 20 min from the start of the reaction according to the Eq. 1.

$PLA_2\ activity = (V_{NaOH} \times c_{NaOH})\ /t$ (Eq.1)

where:

$PLA_2\ activity$ – phospholipase A$_2$ activity [mol of FA released/min],

V_{NaOH} – volume of consumed NaOH solution [dm^3],

c_{NaOH} – concentration of used NaOH solution [mol/dm^3],

t – hydrolysis time [min].

Hydrolysis reactions were carried out in triplicate for each concentration points for both aldehydes.

2.9. Cell culture

HT29 (human colon adenocarcinoma) cell line was purchased from American Type Culture Collection (ATCC). The HT29 cells were maintained in the McCoy's 5A medium supplemented with fetal bovine serum (100 mL/L) and antibiotics: penicillin (100 g/L) and streptomycin (100 U/mL). All reagents for cell culture were purchases from Sigma-Aldrich, Merck KgaA (Darmstadt, Germany). The cells were cultured at 37 °C under humidified atmosphere containing 5% CO$_2$ in a cell incubator (Heal Force, China). For the experiments, the cells derived from passages between 6 and 11 were used. The cells were regularly tested for mycoplasma contamination using Universal Mycoplasma Detection Kit from ATCC.

2.9.1. Preparation of native and oxidized PL/BS mixed micelle solution for cell treatment

14

395 The solutions of native and oxidized PL in SIF (native and oxidized PL/BL mixed micelles) were

396 prepared just before cell treatment. In the case of non-hydrolyzed PL, the samples were incubated in

397 37 °C without addition of PLA$_2$, while the digested samples were subjected to hydrolysis catalyzed by

398 PLA$_2$ (Section 2.7). For the cell treatment purposes, the hydrolysis reaction was stopped after

399 releasing 40 % of the Fas present at the *sn*-2 position of glycerol backbone. Based on the hydrolysis

400 reaction stoichiometry and taking into account the average molecular mass of egg yolk PL (c.a. 752.3

401 g/mol), the mentioned PL hydrolysis degree was achieved after adding 0.8 mL of 0.1 M NaOH solution

402 during pH-stat titration. The PL hydrolysis was terminated by the addition of secretory PLA$_2$ inhibitor –

403 Varespladib (Dennis, Cao, Hsu, Magrioti, & Kokotos, 2011). Based on the preliminary study,

404 Varespladib at the concentration of 5 µM was found to be appropriate for the complete inhibition of

405 porcine pancreatic PLA$_2$. For this purpose, 15 µL of 5 mM Varespladib dissolved in DMSO was added

406 to 15 mL of digestion mixture. To eliminate the differences between samples, this inhibitor was added

407 to non-hydrolyzed samples as well. Additionally, the effect of Varespladib alone on the viability of

408 HT29 cells was determined. The cells were treated with inhibitor at the concentration of 0.5 µM (the

409 final concentration in cell culture medium after addition digestion mixtures in the proportion 9:1. The

410 treatment was carried out for 6, 24, 48 and 72 h. To obtain the PL solutions with different

411 concentrations, non-hydrolyzed and hydrolyzed samples were diluted using SIF (150 mM NaCl, 6 mM

412 CaCl$_2$, 0.28 mM Tris-base, 5 mg/mL BS, pH=8) containing 5 µM Varespladib. The final concentrations

413 of PLs and products of their hydrolysis (LPLs and Fas) in individual samples are shown in

414 **Supplementary Materials (Table A2)**.

415 **2.9.2. Determination of cytotoxicity towards HT29 cells by MTT test**

416 To determined the effect of native and oxidized PL before and after hydrolysis on cell viability, the

417 MTT test was applied as described previously (Baranowska et al., 2018, 2020, 2021). In brief, the

418 exponentially growing HT29 cells were seeded in 96-well cell culture plates (5 × 10^3 cells per well in

419 180 µL of medium) and were allowed to settle for 24 h at 37 °C under 5 % CO$_2$ atmosphere. Then, the

420 cells were treated for 6, 24, 48 and 72 h with 20 µL of different concentrations of native or oxidized PL,

421 before or after *in vitro* intestinal hydrolysis (Table A2). Control cells were treated with the buffer (150

422 mM NaCl, 6 mM CaCl$_2$, 0.28 mM Tris-base, pH=8) or SIF (containing 5 mg/mL of BS mixture). After 6,

423 24, and 48 h of exposure, the medium was aspirated from the wells and replaced with 200 µL of fresh

424 medium. Then, the cells were incubated at 37 °C under 5 % CO$_2$ until 72 h of the total incubation time.

15

425   For the 72 h exposure, the medium was replaced for fresh one at the endpoint. After treatment, 50 μL

426   of MTT solution (4 g/L) was added to all wells and the cells were incubated for another 4 h at 37 °C

427   under 5 % CO_2. Finally, the medium was carefully removed from wells and the formazan crystals

428   formed by metabolically active cells were dissolved in 50 μL of DMSO. The absorbance of the

429   obtained solutions was measured at wavelength of 540 nm and a reference wavelength 690 nm using

430   TECAN Infinite M200 plate reader (Tecan Group Ltd., Switzerland). The differences in absorbance

431   between formazan specific A_{540} and the background A_{690} for individual wells were used for further

432   calculations. Cell treatments were performed as four technical repetitions and three independent

433   repetitions. Cytotoxic effect of tested lipids was expressed as per cent of cell viability compared to

434   control cells treated for 6, 24, 48 or 72 h with 20 μL of the buffer (150 mM NaCl, 6 mM $CaCl_2$, 0.28 mM

435   Tris-base, pH=8) containing 5 μM Varespladib (final concentration in culture medium was 0.5 μM),

436   whose viability was regarded as 100 %. The second type of control constituted cells treated for 6, 24,

437   48 or 72 h with 20 μL of SIF with 5 mg/mL of BS mixture containing 5 μM Varespladib. Results are

438   expressed as means of three independent experiments carried out as four technical replicates.

439   **2.9.3. Determination of genotoxic effect by comet assay**

440   To determine the genotoxic effect of native and oxidized PL before and after hydrolysis in HT29 cells,

441   the comet assay was applied as described previously (Baranowska et al., 2018, 2020, 2021). Briefly,

442   the exponentially growing HT29 cells were seeded in 24-well cell culture plates (10^5 cells per well in

443   1.8 mL of medium) and were allowed to settle for 24 h at 37 °C under 5 % CO_2 atmosphere. Then, the

444   cells were treated for 24 h with 200 μL of two concentrations of native or oxidized PL, before or after *in*

445   *vitro* intestinal hydrolysis (125 and 250 μg/mL) (Table A2). After exposure, the medium was aspirated

446   from the wells and the cells were washed with 0.5 mL of cold PBS, followed by cell detachment with

447   0.2 mL of trypsin solution (0.5 g/L). The addition of 1.8 mL of fresh medium to wells stopped the

448   enzymatic activity of trypsin. Then, 1 mL portions of the cell suspensions were transferred into 1.5 mL

449   tubes and centrifuged (100 × *g*, 5 min, 4 °C). The cell pellets were washed with 1 mL of cold PBS and

450   centrifuged again. PBS was discarded and the cells were resuspended in 150 μL of 0.5 % low-melting

451   point (LMP) agarose. Then, 40 μL of the cell suspension was placed as two spots on a microscope

452   slides covered with normal-melting point (NMP) agarose. The slides were covered with coverslips and

453   placed on an ice-cold tray for at least 5 min to solidify the agarose. After overnight lysis in a high salt

454   alkaline buffer (2.5 M NaCl, 0.1 M EDTA, 10 mM Tris, 1 % Triton X100, pH 10), the slides were placed

16

455   on a Bio-Rad subcell GT electrophoresis platform (Bio-Rad UK), covered with cold electrophoresis

456   buffer (0.3 M NaOH, 1 mM EDTA, pH 13) and chromatin was allowed to unwind for 25 min. Then, the

457   electrophoresis was conducted at 26 V (0.75 V/cm) and 300 mA for 30 min in darkness at 4-8 °C. The

458   slides were transferred to the neutralizing buffer (0.4 M Tris, pH 7.5) for 5 min. This step was repeated

459   twice, then the slides were washed using distilled water and fixed in 70 % ethanol. The DNA was

460   stained using SybrGreen in TE buffer (0.1 Tris-base, 1 mM 1 mM EDTA, pH 10) for 30 min. After

461   staining, the slides were washed in distilled water for 5 min. Finally, the DNA comets were analyzed

462   using fluorescence microscopy (Zeiss ImagerZ2, USA) coupled with a computerized slide scanning

463   system (Metafer4, Germany). Comet analysis involved counting 200 consecutive nuclei per sample.

464   Three slides with two repetitions on each were prepared for each concentration of tested lipid mixture.

465   Genotoxicity of analyzed samples was expressed as the % of DNA in the comet tail relative to total

466   cellular DNA. The control cells were treated for 24 h with 200 µL of the buffer (150 mM NaCl, 6 mM

467    $CaCl_2$, 0.28 mM Tris-base, pH=8) containing 5 µM Varespladib (final concentration in culture medium

468   was 0.5 µM) or SIF with 5 mg/mL of BS mixture containing 5 µM Varespladib. As the positive control

469   served the cells exposed to 150 µM hydrogen peroxide for 1 h.

470   **2.9.4. Visualization of cytosolic lipid droplets**

471   To determine the ability of HT29 cells to accumulate neutral lipids, the cytosolic lipid droplets (CLDs)

472   were visualized according to the method described earlier (Listenberger & Brown, 2007). The

473   exponentially growing cells were seeded in 6-well cell culture plates (4×10^5 cells per well in 3.6 mL of

474   medium) on the bottom of which, the sterile 22 × 22 mm coverslips were placed beforehand. The cells

475   were allowed to settle for 24 h at 37 °C under 5 % CO_2 atmosphere. Then, the cells were treated for

476   24 h with 400 µL of 125 µg/mL test solutions containing native or oxidized PL, before or after *in vitro*

477   intestinal hydrolysis (Table A2). After incubation time, the medium was aspirated from the wells and

478   the cells were washed twice with 2 mL of cold PBS. Then, 2 mL of 4 % formaldehyde in PBS was

479   added to wells and the cells were fixed for 30 min at room temperature. Next, the cells were washed

480   twice with 2 mL of PBS. Immediately before CLD staining, 1 µL of Nile Red stock solution (1 mg/mL) in

481   DMSO was diluted in 10 mL of 150 mM NaCl solution. Next, 1 mL of diluted Nile Red solution was

482   added to all wells. The plates were kept in darkness for 10 min in room temperature, followed by cell

483   washing three times with 2 mL of PBS each. In the next step, the coverslips were mounted onto glass

484   slides using 30 µL of ProLong™ Diamond antifade mountant. Finally, the cytosolic lipid droplets were

17

485 visualized using fluorescence microscopy (Zeiss ImagerZ2, USA). The control cells were treated for

486 24 h with 400 μL of the buffer (150 mM NaCl, 6 mM CaCl$_2$, 0.28 mM Tris-base, pH=8) containing 5 μM

487 Varespladib (final concentration in culture medium was 0.5 μM) or SIF with 5 mg/mL of BS mixture

488 containing 5 μM Varespladib.

489 **2.10. Statistical analysis**

490 Results are expressed as means ± standard deviation (SD) values of three independent experiments

491 unless otherwise stated. An unpaired Student's t-test (p ≤ 0.05) was used to assess the statistical

492 significance of FA composition in PC and PE fractions, PVs and TBARS contents in native and

493 oxidized PL fractions. The statistical significance of the PLA$_2$-catalysed PL hydrolysis rate in different

494 systems and Comet assay results was examined using one-way ANOVA with Tukey's post hoc test.

495 The statistical analysis was performed using the Prism 6.0 software package (GraphPad Software,

496 Inc., USA).

497 **3. Results**

498 **3.1. Characterization of native and oxidized egg yolk PL fractions**

499 **3.1.1. PL class composition**

500 A high purity PL fraction was obtained from hen egg yolk by methanol extraction followed by

501 precipitation of PLs in acetone cooled to −20 °C. The obtained PL fraction contained approximately 5

502 % of non-PL compounds, such as TAGs, Fas and cholesterol, based on total peak areas determined

503 during HILIC-CAD analysis. The same technique confirmed that the most abundant PL classes in hen

504 egg yolk were PCs and Pes, whose amounts were 52.9 % and 30.4 % of total PLs, respectively (Table

505 1). Other PL classes identified were phosphatidylinositols (Pis) and phosphatidylglycerols (PGs),

506 constituting approximately 5 % of total PLs. LPLs, namely lysophosphatidylcholines (LPCs) and

507 lysophosphatidylethanolamines (LPEs) abundance amounted to 2.0 % and 1.5 % of total PLs,

508 respectively. Additionally, sphingomyelins (SMs) were detected in hen egg yolk in the amount of 2.7 %

509 of total PLs.

510 **Table 1. Composition of PL classes present in PL fraction isolated from hen egg yolk.**

PL class (abbreviation)	Composition [% of total peak areas]*
Lysophosphatidylethanolamines (LPEs)	1.54 ± 0.21
Lysophosphatidylcholines (LPCs)	2.03 ± 0.14
Phosphatidylethanolamines (PEs)	30.4 ± 0.6
Phosphatidylglycerols (PGs)	5.08 ± 0.42

Phosphatidylinositols (PIs)	5.32 ± 0.11
Phosphatidylcholines (PCs)	52.9 ± 0.5
Sphingomyelins (SMs)	2.68 ± 0.18

511 * Results are the means of three independent analyses (n=3) ± standard deviation (SD) values.

512 Abbreviation: PL – phospholipid.

513 **3.1.2. FA composition in PC and PE fractions**

514 For a deeper structural analysis of hen egg yolk PLs, the FA composition in the two main PL classes

515 (PCs and PEs), representing over 80 % of total PLs, was determined. For this purpose, the PC and

516 PE classes were separated and isolated by means of preparative TLC, derivatized to FAMEs, and

517 then the FA compositions in each class were determined using GC-FID technique. The results showed

518 statistically significant differences in FA composition between the two analyzed fractions. Saturated

519 FAs (SFAs) accounted for approximately 48 % and 53 % of total FA peak areas in the PC and PE

520 classes, respectively (Table 2). The most abundant FAs in PC species were palmitic acid (16:0) and

521 stearic acid (18:0), whose amounts were 30.3 % and 17.2 % of total FAs, respectively. In contrast, PE

522 fraction was characterised by higher content of stearic acid and lower of palmitic acid. Additionally, in

523 both fractions, myristic (14:0), arachidic (20:0) and behenic (22:0) acids were identified, however, their

524 concentrations were below 1 % of total FAs identified in hen egg yolk PLs.

526 Among the UFAs, in both PC and PE fractions, oleic acid (18:1; n-9) was the most abundant (Table 2).

527 Another notable UFA present in both fractions at significant level was linoleic acid (18:2; n-6), whose

528 concentrations were around 17.4 % and 11.7 % of total FAs, respectively for PC and PE species.

529 Substantial difference between the two fractions was observed for arachidonic (20:4; n-6), and

530 docosahexaenoic acid (22:6; n-3), both of which were more abundant in PE species. In addition, in the

531 structures of both classes, palmitoleic (16:1) and α-linolenic (18:3) were found.

532 **Table 2. Composition of FAs build-in the structure of PC and PE species.**

FA	FA abbreviation	PC fraction	PE fraction
Saturated fatty acids (SFAs) [% of total peak areas]*			
Myristic	14:0	0.14 ± 0.02 [a]	0.41 ± 0.03 [b]
Palmitic	16:0	30.3 ± 0.3 [a]	18.4 ± 0.8 [b]
Stearic	18:0	17.2 ± 1.8 [a]	33.6 ± 2.2 [b]
Arachidic	20:0	0.14 ± 0.01 [a]	0.28 ± 0.01 [b]
Behenic	22:0	0.21 ± 0.01 [a]	0.56 ± 0.03 [b]
Total SFAs		**48.0 ± 1.5** [a]	**53.2 ± 1.5** [b]
Unsaturated fatty acids (UFAs) [%of total peak areas]*			
Palmitoleic	16:1 (n-7)	0.63 ± 0.01 [a]	0.19 ± 0.01 [b]

19

Oleic	18:1 (n-9)	27.6 ± 0.3 [a]	18.4 ± 0.8 [b]
Linoleic	18:2 (n-6)	17.4 ± 1.7 [a]	11.7 ± 0.3 [b]
α-Linolenic	18:3 (n-3)	0.12 ± 0.02 [a]	0.11 ± 0.01 [a]
Arachidonic	20:4 (n-6)	4.1 ± 0.7 [a]	12.0 ± 0.6 [b]
Docosahexaenoic	22:6 (n-3)	1.7 ± 0.4 [a]	3.9 ± 0.2 [b]
Total UFAs		**51.6 ± 1.8** [a]	**46.4 ± 1.5** [b]

533 * Results are the average of three independent analyses (n=3) ± standard deviation (SD) values.

534 Different letters indicate significantly different values examined using unpaired Student's test ($p \leq$

535 0.05).

536 Abbreviations: FA – fatty acid; PC – phosphatidylcholine; PE – phosphatidylethanolamine; SFA –

537 saturated fatty acid; UFA – unsaturated fatty acid.

538 3.1.3. Oxidation level of PL fractions

539 Hen egg yolk PLs were oxidized enzymatically in the presence of sodium deoxycholate using soybean

540 LOX-1. Then, PL oxidation level was estimated using PV and TBARS assays. The first one provides

541 quantitative information on the content of primary lipid oxidation products – lipid hydroperoxides. The

542 other allows to monitor decomposition of lipid peroxidation products. As a result of lipid

543 hydroperoxides decomposition by the C-C bond cleavage, truncated lipids and low-molecular weight

544 volatile aldehydes such as 4-hydroxyhexanal (4-HHE), 4-hydroxynonenal (4-HNE) or MDA are formed.

545 In acidic environment and increased temperature, MDA reacts with thiobarbituric acid (TBA) leading to

546 the formation of MDA-TBA$_2$ adduct that can be quantified. Unfortunately, some other fatty peroxide-

547 derived breakdown products may also react with TBA, giving rise increased result due to false TBA-

548 positive substances (Catalán, Frühbeck, & Gómez-Ambrosi, 2018). The mentioned-above methods

549 were employed for the characterization of PL fraction, both before and after LOX-catalyzed PL

550 oxidation.

552 The enzymatic oxidation catalyzed by LOX is known to cause oxidative modification of UFAs.

553 Accordingly, PV determined for FAs present in the structures of hen egg yolk PLs was statistically

554 significantly higher ($p \leq 0.0001$) compared to native PL fraction (Table 3). In general, PV of fresh lipid

555 fraction (e.g., edible oils) should be below 10 *mEq* O$_2$/kg (Gilbraith, Carter, Adams, Booksh, &

556 Ottaway, 2021), while this parameter determined for oxidized PL fraction exceeded around 30 times

557 the permissible level. This value measured for native fraction indicated that PLs were only slightly

558 modified. The level of TBARS in non-oxidized sample was 0.22 mg/kg, also confirming high quality of

559 the obtained PL fraction. In contrast, the amount of TBARS determined in oxidized PL sample was

560 around 70 times higher ($p \leq 0.0001$) compared to the native PL fraction.

20

561 **Table 3. Peroxide values and TBARS contents in native and oxidized PL fractions.**

Parameters	Native PL fraction	Oxidized PL fraction
Peroxide value [mEq O_2/kg]*	1.3 ± 0.2 [a]	323 ± 22 [b]
TBARS [mg/kg]*	0.22 ± 0.04 [a]	15.3 ± 1.2 [b]

562 * Results are the means of three independent analyses (n=3) ± standard deviation (SD) values.

563 Different letters indicate significantly different values examined using unpaired Student's test (p ≤

564 0.05).

565 Abbreviations: PL – phospholipid; TBARS – thiobarbituric acid reactive substances.

566 **3.2. Characterization of aggregation structures containing native and oxidized PL**

567 In aqueous environment PLs can form aggregation structures with different sizes, such as liposomes,

568 mixed micelles and vesicles or lipid droplets. Because lipid digestion occurs at the oil/water interface,

569 an important factor affecting the kinetics of lipid hydrolysis is the ratio between the surface area of

570 aggregation structures and their volume. Therefore, it is important to characterize the hydrodynamic

571 diameters of obtained aggregation structures before the enzymatic hydrolysis. For this purpose, non-

572 invasive black scatter (NIBS) technique was employed. Its application enabled the determination of

573 aggregation structure size distribution based both on the volume and number of analyzed objects.

574 Additionally, the obtained population was characterized by polydispersity index (PDI) that assess the

575 heterogeneity of the objects based on their size.

576 As a result of ultrasound treatment of PLs dissolved in SIF containing 5 mM BS, a homogeneous

577 population of aggregation structures with an average diameter of 93 nm was obtained (Fig. A1A, Table

578 4). The particles were characterized by a slightly smaller diameter of 67 nm when this parameter was

579 determined based on their number (Table 4). The PDI value of 0.15 confirmed the high homogeneity

580 of the native PL sample.

582 Also for oxidized PLs, using as a basis the object number, the presence of a homogeneous

583 aggregation structure population with an average diameter of 77 nm was found (Table 4). However,

584 different size distribution was observed when the particle diameter was determined by volume (Fig.

585 A1B). In this case, apart from the main object population with diameter of 122 nm, a second

586 population was found with a diameter of 2.8 µm. The latter population accounted for over 35 %

587 aggregation structures analyzed by volume. For this sample, the PDI value was 0.39 that suggest a

588 significantly higher heterogeneity.

590 Furthermore, based on the obtained results, it can be stated that the presence of olive oil TAGs in

591 aggregation structures containing both native and oxidized PLs influenced their size distribution. Using

21

592 the described earlier conditions, the population with hydrodynamic diameter around 56 nm was found

593 for structures containing native PL fraction. Additionally, based on the object number, small population

594 (~ 1 %) of aggregation structures with a size approximately 272 nm was observed (Table 4). A

595 significantly different situation was observed in the size distribution determined by the object volume

596 (Fig. A1C), where the population with a similar hydrodynamic diameter (~ 66 nm) represented only 33

597 %. The main population consisted of aggregation structures with a diameter of approximately 408 nm

598 and accounted for 55 % of the total. Moreover, in the analyzed system, a small population with

599 hydrodynamic diameter of 5,6 µm was detected. The PDI value for the native PL/BS/TAG emulsion

600 was 0.50, which showed the significant influence of TAGs on the increase of heterogeneity of the

601 sample compared to native PL/BS mixed micelle solution (PDI 0.15).

602 Also, the average diameter distribution (based on the object number) of aggregation structures

603 composed of oxidized PLs, BSs and TAGs showed the presence of two populations, the main one

604 with size of 63 nm and a smaller population (< 1 %) with hydrodynamic dimension of 405 nm (Table

605 4). Similarly to the previous sample type (native PL/BS/TAG emulsion), the size distribution measured

606 based on the object volume was significantly different. The structural aggregations with average

607 hydrodynamic dimension of 538 nm were predominant population. Additionally, two other populations

608 of particles were observed: one with diameter of 76 nm and the other with 5.5 µm (Fig. A1D).

609 **Table 4. PDI values and hydrodynamic diameters of aggregation structures PL/BS or**
610 **PL/BS/TAG systems containing native or oxidized PLs.**

System components	PDI*	The size of aggregation structures determined on the basis of			
		Object volumes		Object number	
		Diameter [nm]*	Content [%]*	Diameter [nm]*	Content [%]*
Native PLs + BSs	0.15 ± 0.02	93.0 ± 12.4	100	66.8 ± 1.9	100
Oxidized PLs + BSs	0.39 ± 0.03	122 ± 15	63.2 ± 15.7	77.0 ± 5.9	100
		2784 ± 693	36.8 ± 9.3	-	-
Native PLs + BSs + TAGs	0.50 ± 0.08	408 ±118	55.3 ± 4.7	55.9 ± 9.3	99.6 ± 0.5
		66.0 ± 14.0	33.3 ± 8.6	272 ± 23	0.78 ± 0.29
		5579 ± 216	4.0 ± 2.0	-	-
Oxidized PLs + BSs + TAGs	0.57 ± 0.09	538 ± 160	67.5 ± 6.9	62.6 ± 10.9	99.3 ± 0.2
		75.7 ± 25.0	31.6 ± 7.4	405 ± 82	0.69 ± 0.20
		5489 ± 99	2.6 ± 1.0	-	-

611 * Results are the means of five independent determinations (n=5) ± standard deviation (SD) values.

612 Abbreviations: BS – bile salt; PDI – polydispersity index; PL – phospholipid; TAG – triacyloglicerol.

22

3.3. PLA$_2$-catalysed hydrolysis of native and oxidized PLs embedded in mixed micelles and emulsions

Kinetics of PLA$_2$-catalysed hydrolysis of native and partially oxidized PLs present in mixed micelles or emulsions was determined using pH-stat method. This approach enabled monitoring of enzymatic hydrolysis of lipids based on the volume of NaOH solution used for neutralization of released FAs to maintain the pH at a constant value (pH=8 in this case) (Beisson, Tiss, Rivière, & Verger, 2000). Among all tested sample types, the native PL/BS mixed micelles were the most liable to hydrolysis catalyzed by PLA$_2$. After 10 min from the initiation of hydrolysis by the addition of PLA$_2$, approximately 26.4 mol % of FAs present in *sn*-2 position of PLs were released. In this period, the reaction proceeded at the highest rate (Fig. 2). The amounts of FAs released after 30 and 60 min were respectively 43.4 and 54.7 mol %, which clearly showed that the hydrolysis rate decreased with the reaction time. The addition of olive oil TAGs led to slight decrease of PL hydrolysis catalyzed by PLA$_2$. However, the differences in hydrolysis rate between native PL-containing systems without and with TAGs were not statically significant over the entire hydrolysis time range.

Oxidation of UFAs found in the structure of PLs caused a statistically significant slowdown of hydrolysis of oxPL/BS mixed micelles catalyzed by PLA$_2$. The discrepancy between hydrolysis rate of native and oxidized PL was growing especially in the range of 2 – 20 min. The amount of FAs released after 10 min of the reaction amounted to 20.2 mol % of FAs present in the *sn*-2 position of oxPLs, while this parameter achieved the value of 33.2 and 43.1 mol % after 30 and 60 min, respectively. For the oxPL/BS/TAG emulsion sample, the lowest digestibility by PLA$_2$ was observed. Similarly to the emulsion containing native PLs, the addition of olive oil TAGs slightly decreased the PL hydrolysis rate in oxPL/BS/TAG system, compared to mixed micelles with oxidized PL fraction. However, in these cases, the effect of TAG addition made statistically significant difference ($p \leq 0.05$) beginning from 40 min of the reaction. After 10 min of the hydrolysis, approximately of 18.6 mol % of FAs were released. Longer hydrolysis times (30 and 60 min) resulted in 30.2 and 39.0 mol % of FAs released from the *sn*-2 position of PLs, respectively.
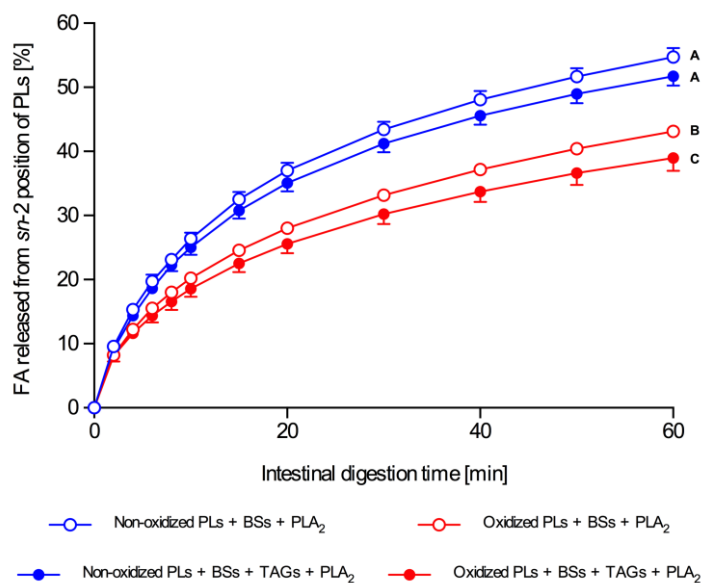
640

641 **Fig. 2.** PLA₂-catalysed hydrolysis of native and oxidized PL in the aggregation structures of mixed

642 micelles and emulsions. The results are the average of three independent analyses (n=3). For the

643 sake of legibility of the drawing, the standard deviation (SD) values in the graph is presented in one

644 direction only (plus or minus). In the curve for oxidized PLs + BSs + PLA₂, the SD values were smaller

645 than the symbol size used. Different letters at the endpoint of hydrolysis time indicate significantly

646 different values examined using one-way ANOVA with Tukey's post hoc test ($p \leq 0.05$).

647 (Abbreviations: BS – bile salt; FA – fatty acid; PL – phospholipid; PLA₂ – phospholipase A₂; TAG –

648 triacyloglicerol)

649 **3.4. Impact of hexanal and (*E*)-2-nonenal on PLA₂ activity**

650 As mentioned earlier, low-molecular weight volatile aldehydes are formed as a result of degradation of

651 lipid hydroperoxides by the cleavage of the C-C bond in UFA chains. Due to the frequent occurrence

652 of linoleic acid in the structure of hen egg yolk PLs and its relatively high oxidability, hexanal was

653 found to be one of the most abundant aldehydes among the volatile compounds identified in the

654 headspace of the hen egg yolk PL fraction heated for 20 min at 100 °C (Chen, Balagiannis, & Parker,

655 2019). Another type of volatile aldehydes that are formed during lipid oxidation are electrophilic α-β-

656 unsaturated aldehydes, which are susceptible to nucleophilic attack at the β-carbon position. The most

657 abundant α-β-unsaturated aldehydes identified in the hen egg yolk PL fraction exposed to elevated

658 temperature were (*E*)-2-heptenal, (*E*)-2-octenal, (*E*)-2-decenal and (*E*)-2-nonenal (Chen et al., 2019).

659 In order to determine the effect of low-molecular volatile aldehydes on PLA₂ activity, two of those

24

660   aldehydes were used: hexanal and (*E*)-2-nonenal. The IC_{10} and IC_{30} values for both studied aldehydes

661   are shown in Table 5.

663   The obtained IC_{10} and IC_{30} values were lower for (*E*)-2-nonenal compared to the saturated aldehyde –

664   hexanal (Table 5). Importantly, in the case of both tested aldehydes – hexanal and (*E*)-2-nonenal–

665   further increase in concentrations (above ~ 20 mM) did not lead to a linear decrease in the PLA_2

666   activity. Therefore, a 50 % reduction in enzyme activity was not achieved and consequently the IC_{50}

667   values for neither of these aldehydes could be determined.

668   **Table 5. Inhibitory concentration (IC) values determined for studied aldehydes causing 10 %**

669   **and 30 % inhibition of porcine pancreatic PLA_2 activity.**

| Aldehyde	IC_{10} [mM]*	IC_{30} [mM]*
Hexanal	5.2 ± 0.6	15.7 ± 1.8
(*E*)-2-nonenal	3.3 ± 0.4	13.3 ± 1.5

670   * Results are calculated based on the equation of aldehyde concentration vs. percentage of PLA_2

671   inhibition in the linear range. All concentration points (0, 5, 10, 15, 20 mM) were determined in

672   triplicate (n=3) ± standard deviation (SD) values for each aldehyde.

673   Abbreviation: PLA_2 – phospholipase A_2.

674   **3.5. Impact on cell viability**

675   The impact of native and oxidized PLs on HT29 cell viability was assessed using MTT test. The HT29

676   cell line was chosen as a model of the intestinal epithelium tissue that comes into direct contact with

677   ingested food components. This cell line is recommended for nutritional studies i.a. by the National

678   Centre for the Replacement, Refinement and Reduction of Animals in Research (UK) (Krishna &

679   Gopalakrishnan, 2016) and a detailed explanation of the reason for choosing this cell line is presented

680   in the section 1. Since earlier studies indicated that part of food-delivered PLs could be absorbed by

681   intestinal cells without their prior hydrolysis (Zierenberg & Grundy, 1982), the cells were exposed to

682   native and oxidized PLs in the presence of BS, both before and after intestinal hydrolysis. In the

683   present study, two types of control cell cultures were used. The first one involved HT29 cells treated

684   with the buffer (150 mM NaCl, 6 mM $CaCl_2$, 0.28 mM Tris-base, pH=8). The second type of control

685   constituted of HT29 cells exposed to SIF that contained BS mixture at the concentration of 500 µg/mL.

686   BSs are important surface-active compounds responsible for solubilization of food-delivered lipids,

687   which enables their effective hydrolysis. Therefore, they are essential components of SIF used during

688   *in vitro* intestinal digestion studies. In our study, BS mixture was used during lipolysis on native and

689   oxidized PL fractions at the concentration of 5 mg/mL. However, the final concentration of BS mixture

25

690   in culture medium containing native or oxidized PLs before or after intestinal hydrolysis was 500

691   µg/mL. Additionally, the culture medium contained 0.5 µM Varespladib, which inhibits the PLA$_2$-

692   catalyzed hydrolysis of PLs. The inhibitor was added to all types of cell cultures, including controls and

693   cells exposed to non-hydrolyzed PLs, to eliminate its influence on cell viability while comparing

694   treatments with different samples. The preliminary studies showed that Varespladib was not cytotoxic

695   at the concentration used. Dose-response curves after 6, 24, 48 and 72 h of cell exposure to native

696   and oxidized PLs before and after hydrolysis are shown in **Fig. 3**. Results of the statistical analysis are

697   available in the Supplementary Materials (Table A3).
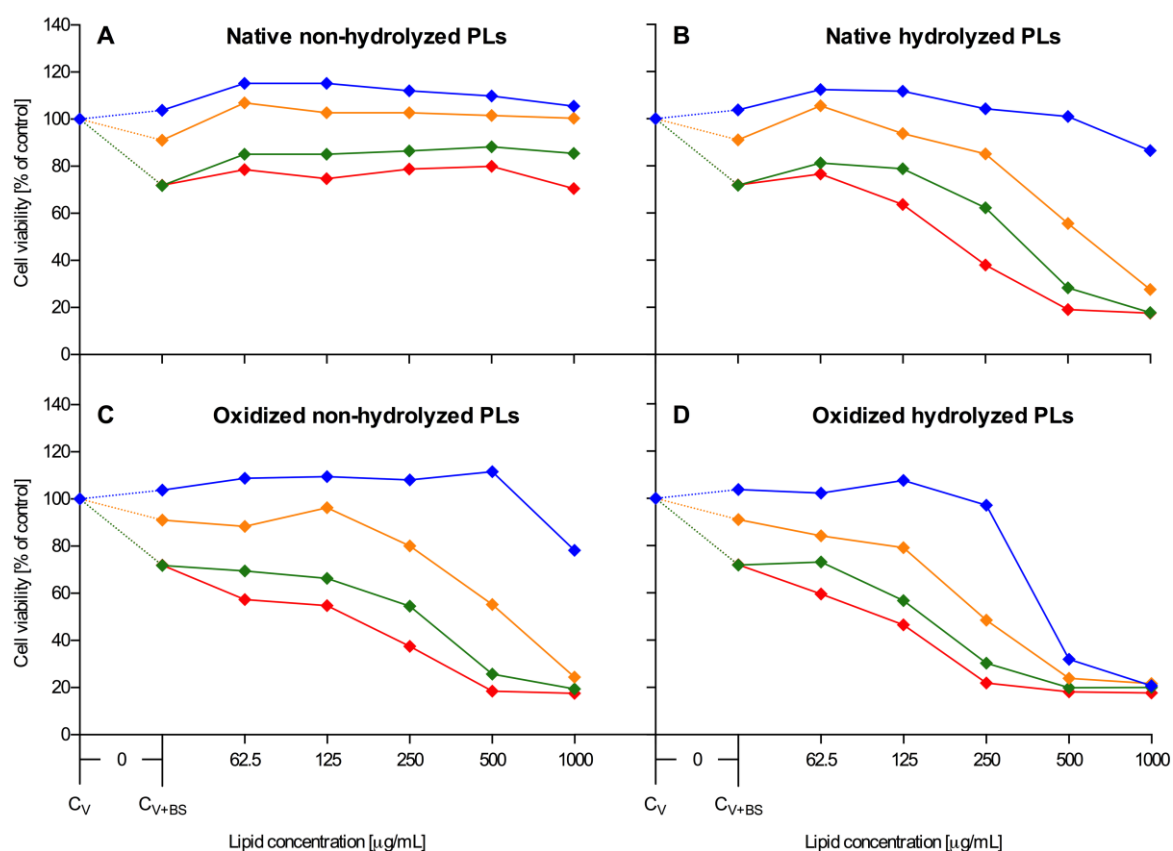
698

699   **Fig. 3.** Cell viability of HT29 cells determined by MTT test after 6 (blue), 24 (orange), 48 (green) and

700   72 h (red) exposure to: native non-hydrolyzed PL/BS mixed micelle solution (A); native hydrolyzed

701   PL/BS mixed micelle solution (B); oxidized non-hydrolyzed PL/BS mixed micelle solution (C) and

702   oxidized hydrolyzed PL/BS mixed micelle solution (D). Results represent means of three independent

703   experiments carried out in quadruplicate (standard deviation (SD) values are lower than 15 %).

704   Results of statistical analysis are available in Supplementary Materials (Table A3). (Abbreviations: BS

705   – bile salt; C_V – control cells treated with buffer containing 0.5 µM Varespladib; C_{V+BS} – control cells

706 treated with SIF containing 500 µg/mL BSs and 0.5 µM Varespladib; PL – phospholipid; SIF –

707 simulated intestinal fluid)

708 The exposure of HT29 cells to SIF containing only a BS mixture led to the decrease of their viability

709 (Fig. 3). This effect was observed especially for prolonged treatment times (48 and 72 h), for which the

710 decrease of cell viability was around 30 %, while for 24 h the cell viability achieved around 90 %

711 compared to control cells exposed to buffer only. Importantly, the simultaneous presence of native

712 non-hydrolyzed PLs, across the range of concentrations used (62.5 – 1000 µg/mL), led to a reversal of

713 the cytotoxic effect of BS for all tested exposure times (Fig. 3A). Additionally, there was no significant

714 effect of the increasing PL concentration on cell viability. However, it was observed that the prolonged

715 exposure times (48 and 72 h) decreased the viability of the cells compared to the control ones treated

716 with buffer only..

717 PL digestion catalyzed by PLA_2 leads to the formation of 1-LPL and FA. In our experiments, after

718 releasing 40 % of the FAs present at the *sn*-2 position of PL, the reaction was terminated by the

719 addition of PLA_2 inhibitor Varespladib. For this sample type, containing native PL and product of their

720 lipolysis, the reduction of the cytotoxic effect of BS was observed in the case of the lowest lipid

721 concentration used (62.5 µg/mL) for all tested exposure times (Fig. 3B). However, the protective effect

722 was not observed for higher concentrations (125 – 1000 µg/mL). For the shortest incubation time (6 h),

723 only the highest concentration tested (1000 µg/mL) caused a decrease in cell viability by about 15 %

724 compared to the buffer-treated control cells. While, for exposure times of 24, 48 and 72 h, there was a

725 significant dose-dependent decrease in HT29 cell viability with an increase in the concentrations of

726 PLs and products of their hydrolysis (1-LPL and FA) in the tested mixtures containing constant BS

727 concentration.

728 The oxidative modification of PL significantly contributed to the viability of HT29 cells compared to

729 their native counterparts (Fig. 3C). In the case of the shortest incubation time (6h), no significant

730 decline in HT29 cell viability was observed in the concentration range of 62.5 – 500 µg/mL. However,

731 the cell exposure to the highest concentration of oxidized PL at the same incubation time (6 h) led to a

732 20 % decrease of cell viability. For longer exposure times in the range of 24 – 72 h, negative

733 correlation between oxidized PL concentrations and cell viability was observed. A significant decrease

734 in cell viability , for these treatment times, was observed for all concentrations above 125 µg/mL.

735 Furthermore, for this sample type, no significant protective effect against BS-induced cytotoxicity was

736 observed.

737 The oxidized PLs after their partial hydrolysis (around 40 % of total PL) were characterized by the

738 highest cytotoxicity among all tested samples (Fig. 3D). For the incubation time of 6 h, no significant

739 decrease in HT29 cell viability was observed in the concentration range of 62.5 – 250 µg/mL. Above

740 this range, a sharp decrease in cell survival was observed, reaching around 70 % decline in cell

741 viability for concentration of 500 µg/mL. For the incubation times of 24, 48 and 72 h, negative

742 correlation between lipid (PL/1-LPL/FA) concentrations and cell viability was observed. For 24 and 48

743 h exposure times, maximum reduction of cell viability was observed for concentrations of 500 and

744 1000 µg/mL, while for 72 h the maximum viability decrease was achieved for consternations above

745 250 µg/mL. Similarly to oxidized non-hydrolyzed PLs, the protective effect against cytotoxicity induced

746 by BS mixture was not observed for oxidized PL fraction after partial hydrolysis.

747 **3.6. Genotoxicity**

748 The effect of native and oxidized PL before and after hydrolysis on the DNA integrity of cells treated

749 for 24 h with tested samples was determined by a comet assay. The test is based on the detection of

750 DNA strand breaks in single cells embedded in LMP agarose (single-cell gel electrophoresis test). The

751 lipid concentrations used in the comet assay (125 and 250 µg/mL) were selected on the basis of the

752 results obtained by MTT test, so that the viability of HT29 cells treated for 24 h with the tested

753 solutions was not lower than 80 % of control cell viability. The only exception was the cells exposed to

754 oxidized PL/BS mixed micelles after partial hydrolysis, where the cell viability was inhibited by about

755 50 % for the concentrations of 250 µg/mL.

756 Among all tested samples, the treatment with BS mixture alone at the concentration of 500 µg/mL

757 caused the highest genotoxicity (Fig. 4). Interestingly, the BS-induced the genotoxic effect was similar

758 to DNA damage observed in the case of positive control cells treated with 150 µM H_2O_2 for 1 h. The

759 percentage of DNA in tail for these samples was 21.2 and 26.5 %, respectively. On the other hand, the

760 obtained results indicated that the simultaneous presence of PLs, either native or oxidized before and

761 after hydrolysis at both tested concentrations (125 and 250 µg/mL), significantly reduced BS-induced

762 DNA fragmentation. Moreover, for most of the tested sample types, a statistically significant difference

763 in DNA integrity was observed between the two applied concentrations, with 250 µg/mL offering better

764 protection. The statistical analysis does not confirm concentration dependence only for native non-

28

hydrolyzed PL, for which the p value was 0.1148. Overall, however, the same effect on BS-induced

genotoxicity was observed regardless of PL oxidation or hydrolysis.
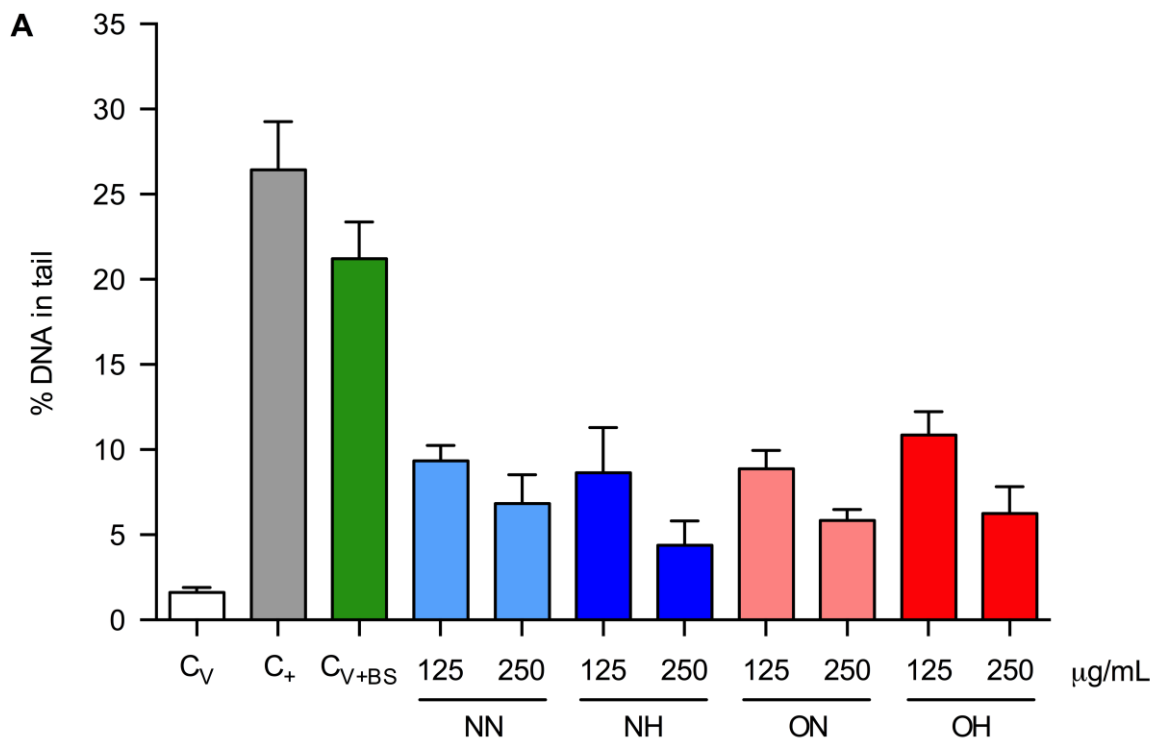
| vs.	C+	C_V+BS	NN 125	NN 250	NH 125	NH 250	ON 125	ON 250	OH 125	OH 250
C_V	<0.0001	<0.0001	<0.0001	0.0001	<0.0001	0.0577	<0.0001	0.0010	<0.0001	0.0002
C+		<0.0001	<0.0001	<0.0001	<0.0001	0.0195	<0.0001	<0.0001	<0.0001	<0.0001
C_V+BS			<0.0001	<0.0001	<0.0001	<0.0001	< 0.0001	<0.0001	<0.0001	< 0.0001
NN 125				0.1148	0.9987	<0.0001	>0.9999	0.0040	0.7845	0.0183
NN 250					0.5527	0.1471	0.3725	0.9861	0.0004	0.9998
NH 125						0.0002	>0.9999	0.0541	0.2484	0.1722
NH 250							<0.0001	0.8107	<0.0001	0.5039
ON 125								0.0251	0.4020	0.0912
ON 250									<0.0001	>0.9999
OH 125										<0.0001

Fig. 4. Genotoxic effects of native and oxidized PL/BS mixed micelles before and after hydrolysis

determined in HT29 cells by comet assay and expressed as % DNA in the comet tail (Panel A).

Results represent means of three independent experiments and standard deviation (SD) values. In the

graph, the SD values are presented only in the plus direction. The final concentration of PLA$_2$ inhibitor

in cell medium for all tested samples was 0.5 µM. Probability values for individual sample pairs were

compared using one-way ANOVA with Tukey's post hoc test. Values with statistically important

difference ($p < 0.05$) between the two compared samples are marked in bold red, while probability

values $p \geq 0.05$ in normal font (panel B). (Abbreviations: BS – bile salt; C$_+$ – positive control cells

776 treated with 150 μM H_2O_2 for 1 h; C_v – control cells treated with buffer containing 0.5 μM Varespladib;

777 C_{v+BS} – control cells treated with SIF containing 500 μg/mL BSs and 0.5 μM Varespladib; NH – native

778 hydrolyzed; NN – native non-hydrolyzed; OH – oxidized hydrolyzed; ON – oxidized non-hydrolyzed;

779 PL – phospholipid; PLA_2 – phospholipase A_2; SIF – simulated intestinal fluid)

3.7. Neutral lipid accumulation

781 CLDs are intracellular organelles composed of a core containing neutral lipids (mainly TAGs)

782 surrounded by a PL monolayer with various proteins embedded in it. CLDs can be visualized using

783 fluorescence microscopy after staining of CLDs with lipophilic dye – Nile Red. In a neutral lipid

784 environment (e.g., CLD core), Nile Red exhibits green fluorescence with a maximum emission at the

785 wavelength of 585 nm (excitation wavelength of 510 nm). In contrast, in PL-rich structures (e.g.,

786 cellular membranes), Nile Red exhibits red fluorescence with emission and excitation wavelengths of

787 640 and 550 nm, respectively. In the present study, the accumulation of natural lipids in CLDs was

788 assessed using the green fluorescence of Nile Red (Listenberger & Brown, 2007). Before CLD

789 imagining, HT29 cells were treated for 24 h with native or oxidized PL/BS mixed micelles (125 μg/mL)

790 before and after hydrolysis catalyzed by PLA_2.

791 Visual analysis of the fluorescence intensity of CLDs present in HT29 cells suggested that the

792 presence of free FA increases the accumulation of neutral lipids since it was significantly higher for

793 native and oxidized PL/1-LPL/FA mixture compared to non-hydrolyzed PLs (Fig. 5). There was

794 however no effect of PL oxidation on fluorescence intensity, which indicates no increase in the

795 accumulation of neutral lipids. No differences were observed, between cells exposed to non-

796 hydrolyzed both native or oxidized PLs and control cells treated with the buffer (150 mM NaCl, 5 mM

797 $CaCl_2$, 0.28 mM Tris) containing 5 μM Varespladib. Additionally, based on the visual analysis, there

798 was no influence of BS mixture (500 μg/mL) on lipid accumulation.
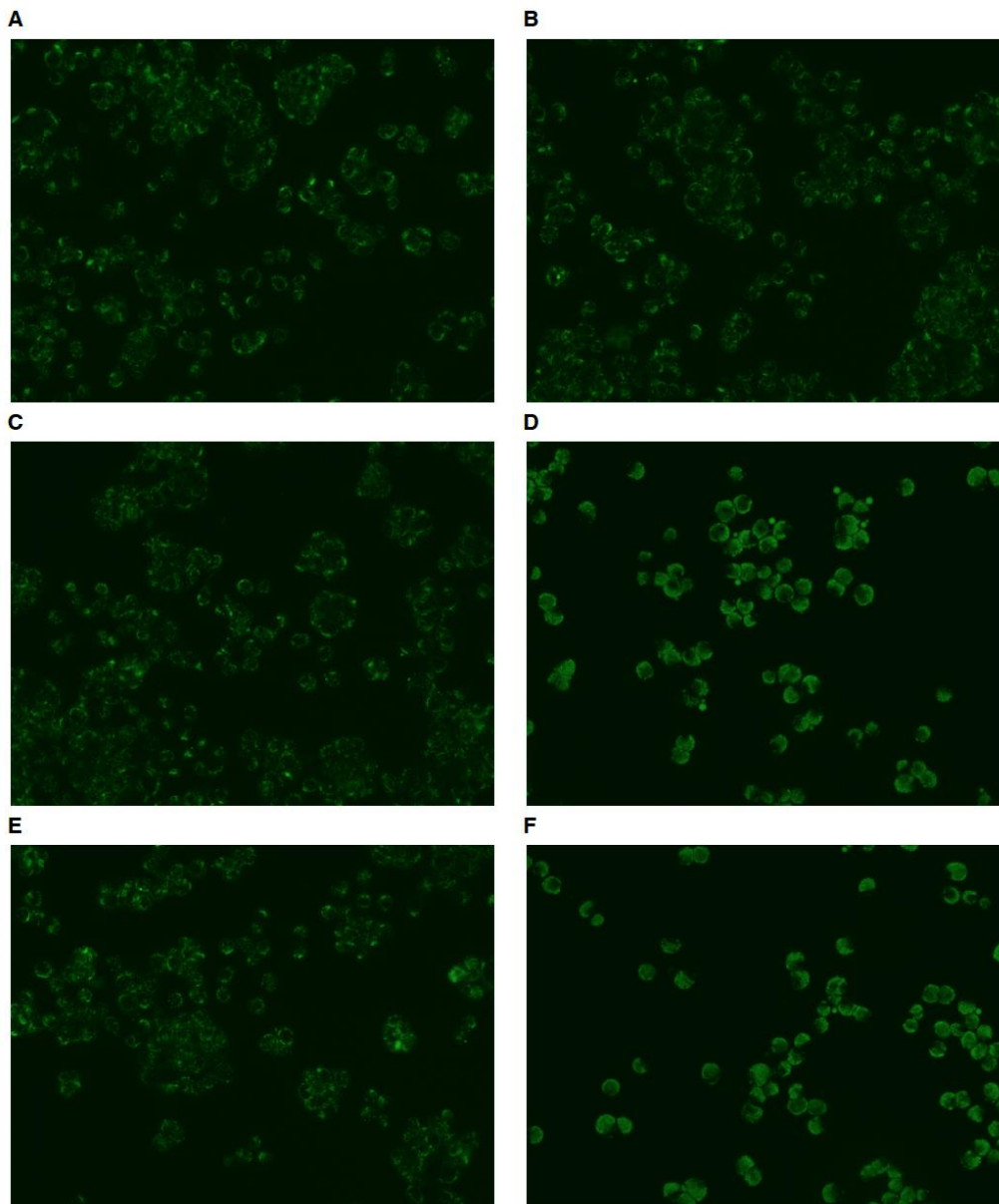
Fig. 5. Visualization of CLDs in HT29 cells after 24 h exposure to PL/BS mixed micelles intact or submitted to PLA$_2$ catalyzed hydrolysis using fluorescent microscopy and Nile Red staining: cells treated with buffer containing 0.5 µM Varespladib (A); cells treated with SIF containing 500 µg/mL BSs and 0.5 µM Varespladib (B); cells treated with native PL/BS mixed micelle solution (C); cells treated with native PL/BS mixed micelle solution after hydrolysis (D); cells treated with oxidized PL/BS mixed micelle solution (E) and cells treated with oxidized PL/BS mixed micelle solution after hydrolysis (F). The final concentrations of PL and BS in cell medium containing mixed micelles were 125 and 500 µg/mL, respectively. (Abbreviations: BS – bile salt; CLD – cytosolic lipid droplet; PL – phospholipid; PLA$_2$ – phospholipase A$_2$)

4. Discussion

810 Oxidative modifications of FAs found in the structure of lipids lead to the loss of the nutritional value

811 and deterioration of sensory properties of food products (Jacobsen, Paiva-Martins, Schwarz, &

812 Bochkov, 2019). Moreover, a variety of harmful substances can be formed, including lipid

813 hydroperoxides and products of their decomposition, containing hydroxy, epoxy, keto or aldehyde

814 groups. It has been estimated that daily intake of LOOHs is around 1.5 mmol (Kanner, 2007). While

815 the consumption of acrolein (α-β unsaturated aldehyde formed from PUFAs via LOOHs) can

816 significantly exceed 1 mg per day (according to some data the maximum exposure is 0.1 mg/kg/day

817 (Henning, Johnson, Coyle, & Harbison, 2017; Vieira, Zhang, & Decker, 2017)), which is far above the

818 Tolerable Daily Intake (TDI) value of 7.5 µg/kg/day recommended by the World Health Organization

819 (WHO) (Jiang et al., 2022). Unfortunately, general health recommendations for the maximum

820 acceptable human daily intakes (MHDIs) of other LOPs are either extremely limited or completely

821 unavailable (Grootveld, Percival, Leenders, & Wilson, 2020).

822 An in $vivo$ study in a rat model fed with non-oxidized and oxidized (PVs in the range of 100 – 1200

823 mEq O_2/kg) soybean oils indicated that animal exposure to oils with PVs above 400 mEq O_2/kg

824 significantly decreased weight gain compared to the control group. A diet containing oxidized oil with a

825 PV of 1200 mEq O_2/kg caused deaths within the approximately three weeks. Among the symptoms,

826 weight loss during the experiment and severe diarrhea were observed. Animals fed with oil

827 characterized by PV of 800 mEq O_2/kg developed moderate to severe diarrhea, but the symptom had

828 subsided somewhat by the eighth week. Additionally, the histological examinations of the animals fed

829 with highly oxidized fraction (PV above 3000 mEq O_2/kg) indicates that intestines were one of the most

830 affected organs and were characterized by the presence of cytoplasmic vacuoles distending mucosal

831 (Andrews, Griffith, Mead, & Stein, 1960). Cases of food poisoning manifested by acute symptoms

832 such as diarrheal, nausea, emesis, abdominal pain, fatigue, and headache, were also observed in

833 humans consuming processed foods containing oils and fats with PVs of at least 100 mEq O_2/kg

834 (Gotoh et al., 2006). Moreover, chronic consumption of such foodstuffs has been postulated to

835 increase the risk of disorders such as alimentary tract cancers, cardiovascular diseases and nervous

836 system disorders (neurotoxicity) (Gotoh et al., 2006; Jackson & Penumetcha, 2019). Therefore, it

837 seems important to understand the influence of oxidation of dietary lipid on important physiological

838 processes occurring in the intestinal lumen, namely digestion and up-take as well as the subsequent

839 biological effects of lipid oxidation and hydrolysis towards IECs.

840   To address these questions, in the present study, we used PL fraction isolated from hen egg yolk that

841   is the main nutritional source of PLs in typical Western diet (Blesso, 2015). As shown in Table 2, hen

842   egg yolk PL species contained a significant share of UFAs, including PUFAs such as α-linolenic or

843   arachidonic acids. Therefore, PL fraction isolated from egg yolk was selected as a suitable model for

844   oxidation and further assessment of its impact on IECs. In general, oxidized lipids can be formed in

845   three ways: by non-enzymatic autoxidation and photo-oxidation or *via* enzyme-catalysed reaction, but

846   all of these reactions lead to the formation of lipid hydroperoxides as primary oxidation products

847   (Domínguez et al., 2019). However, to ensure a high yield of PL oxidation needed in our study, the

848   LOX-catalysed reaction was chosen. The PV determined for oxidized PL fraction (323 *mEq* O_2/kg)

849   confirmed that PL species were oxidized with high efficiency and could be successfully used in further

850   stages of our research (Table 3). Our previous analysis, using two-step high-performance liquid

851   chromatography (HPLC) coupled with mass spectrometry (MS) technique, confirmed the presence of

852   not only PL hydroperoxides, but also PL dihydroperoxides in the LOX-catalysed hen egg PL fraction

853   (Parchem, Kusznierewicz, et al., 2019). The latter are not typical lipid oxidation products, however,

854   previous studies indicated that they can be formed *in vitro* at high enzyme concentration (Brash,

855   1999). Additionally, lipid dihydroperoxides were detected in virgin and refined soybean oils exposed to

856   elevated temperature (70°C) (Martin-Rubio, Sopelana, Ibargoitia, & Guillén, 2021). Our current study

857   also showed a statistically significant difference in TBARS content between oxidized and native

858   fraction (Table 3). This indicated at least a partial decomposition of full-chain length PL

859   (di)hydroperoxides by C-C bond cleavage and formation of low-molecular weight aldehydes, known to

860   inhibit pancreatic PLA_2 activity, and thereby obstructing PLs hydrolysis (Litvinko et al., 2018).

861   In the next step of the study, the effect of PL oxidation on the parameters of aggregation structures

862   present in SIF containing BS mixture was evaluated. In general, PLs can form different aggregation

863   structures, whose spatial organization depends on the presence and composition of surfactants (e.g.,

864   BSs), other lipid molecules (e.g., TAGs), non-lipid compounds (e.g., proteins) as well as on

865   physicochemical properties of aqueous phase (Birru et al., 2014; Meyuhas et al., 1997). Under the

866   conditions used in our study, native PLs formed the homogeneous population of aggregation

867   structures. Taking into account their size (67 and 93 nm based on the object number and volume,

868   respectively), it can be assumed that the PL/BS mixed micelles or/and vesicles were obtained. The

869   typical size of mixed micelles, based on the literature data, ranges from 50 to 150 nm (Riethorst et al.,

870   2016), while this parameter for mixed vesicles achieves values from 50 to several hundred nm (Birru

871   et al., 2014), though unequivocal identification of aggregation structure type is not possible only on the

872   basis of their size. In this study, the obtained aggregation structures are referred to as mixed micelles,

873   however, noted that unambiguous identification was not made in this study. The size distribution of

874   native PL/BS sample (Fig. A1A) indicated also the presence of structures with the diameter below 50

875   nm, which are most likely single-component BS micelles. Their typical size ranges from 10 to 50 nm

876   (Riethorst et al., 2016). The replacement of native PLs by their oxidized counterparts led to slightly

877   increased hydrodynamic diameter of the structures formed (Table 4, Fig. A1B). This can result from

878   the displacement of oxidized FAs present in surface PLs from hydrophobic part of the aggregation

879   structure towards the aqueous environment, which is related to the increased hydrophilicity of FAs due

880   to their oxidative modification. Consequently, the hydrophilic groups of oxidized FAs could interact with

881   water molecules leading to the formation of solvation shell and increase in hydrodynamic diameter.

882   The presence of oxidized FAs on the liposome surface has also been suggested in previous studies,

883   in which a model composed of cholesterol and PC species with hydroperoxy linoleic acid was applied

884   (Kambayashi, Yamamoto, & Nakan, 1998). Moreover, the size distribution of the oxidized PL/BS

885   structures determined by volume revealed not only the major population with the hydrodynamic

886   dimension of 122 nm, but also another fraction with a much larger dimension of 2.8 μm. This could be

887   a result of the aggregation of the primary structures into larger clusters *via* e.g., cross-linking of PL

888   molecules by imine formation. Such reaction is known to occur between the primary amines found in

889   the PE head group (ethanolamine) and the aldehyde groups. The latter can be present in the structure

890   of truncated oxPL formed by C-C bond cleavage along UFA acyl chain. Importantly, oxidation of PLs

891   followed by imine formation was reported as a necessary step in sphingosine-induced vesicles

892   aggregation (Jiménez-Rojo et al., 2014).

893   The addition of olive oil TAGs to native and oxidized PL/BS systems resulted in significant changes of

894   the size distributions based on object volume compared to TAG-free systems (Fig. A1). For native

895   PLs, a heterogeneous system was obtained with the main population characterised by hydrodynamic

896   diameter of 408 nm. It may be postulated that lipid droplets were formed under the conditions used.

897   Their typical size, according to literature data, ranges from 20 to 500 nm for lipid droplets forming

898   nanoemulsion, while aggregation structures with dimension of 1 – 100 μm are typical for

899   macroemulsions (A. Gupta, Eral, Hatton, & Doyle, 2016). Additionally, the lipid droplets with the size

900 specific for macroemulsions (5.6 µm) were also observed in our system. However, their share was

901 small and accounted for about 4% based on particle volume. The second most abundant population in

902 the analyzed system were aggregation structures with the size below 100 nm, which corresponds to

903 small lipid droplets present in nanoemulsion (A. Gupta et al., 2016). Importantly, these structures

904 represented a practically homogeneous population when the size distribution was based on the object

905 number. Similarly to PL/BS models, the use of oxidized PLs had a slight effect on the size distribution

906 of the structures composed of PLs, BSs and TAG compared to native ones. Most likely this was

907 associated with changes in spatial structure and physicochemical properties of PL species containing

908 oxidized FAs that affected their behaviour during the assembly of the aggregation structures.

909 Although the addition of olive oil TAGs to the system containing native PLs and BS mixture affected

910 the size distribution of formed aggregation structures, no effect was observed on the PL hydrolysis

911 catalyzed by pancreatic PLA_2. This suggested that in both analyzed systems (without and with TAGs),

912 the enzyme had an unimpeded access to the substrates located on the surface of aggregation

913 structures. In contrast, a significant decrease in the hydrolysis rate was observed for the systems

914 containing oxPLs, especially in the model containing additionally TAGs. As already mentioned, PL

915 hydroperoxides are preferentially hydrolyzed by PLA_2 compared to the native counterparts, at least

916 when standard PC hydroperoxide (PC18:0/18:2(-OOH)) was used (Baba et al., 1993). In contrast,

917 another study suggested that UV-irradiation of hen egg yolk PL/sodium deoxycholate mixed micelles

918 decreased porcine pancreatic PLA_2 activity after 40 min of the reaction. In this case, however, the

919 authors linked their observation to significant increase of MDA level formed over this time (Litvinko et

920 al., 2018). Therefore, in our study we have attempted to determine the effect of low-molecular

921 aldehydes on the porcine pancreatic PLA_2 activity.

922 The chemical structures of formed aldehydes depend on the structure of precursor UFA (e.g., n-6 or n-

923 3 family) and the oxidation pathway. In general, saturated and α-β-unsaturated aldehydes, can be

924 distinguished. In our study, we determined the effect of hexanal and (*E*)-2-nonenal – representatives

925 of saturated and unsaturated aldehydes, respectively, previously identified in the hen egg yolk PL

926 fraction exposed to elevated temperature (Chen et al., 2019) – on PLA_2 activity. The obtained data

927 indicated that both tested aldehydes showed the ability to inhibit this enzyme with (*E*)-2-nonenal being

928 more effective inhibitor of PLA_2 activity (Table 5). Aldehydes can covalently modify enzymes by

929 electrophilic addition to primary amines of the amino acids, such as lysine and arginine, with the

35

930   formation of Schiff's bases. Porcine pancreatic PLA_2 (1SFW according to the PDB database) is a

931   small enzyme composed of 124 amino acids. Its active side includes His-48, Asp-99 and Ca^{2+} ion that

932   is bound by Tyr-28, Gly-30, Gly-32, Asp-49. Additionally, PLA_2 structure is stabilized by seven disulfide

933   bonds, which makes this enzyme highly resistant to chemically and thermally induced unfolding

934   (Kölbel, Weininger, Ihling, Mrestani-Klaus, & Ulbrich-Hofmann, 2015). However, there are nine lysine

935   and four arginine residues in the amino acid sequence of PLA_2 that may be modified by the mentioned

936   aldehydes, which can cause the change in the enzyme conformation and lower its activity. As

937   described earlier, for both tested aldehydes, the reduction of enzymatic activity by 50 % could be not

938   achieved, despite the increases in aldehyde concentration. This explanation could be that after

939   reaching a certain aldehyde concentration, all possible liable to modification enzyme sites become

940   modified, leading to a decrease in its activity, but not complete inactivation. Therefore, an increase in

941   the aldehyde concentration did not cause further reduction of enzymatic activity.

942   Summarizing this part of the work, it can be stated that oxidation of dietary (phospho)lipids, and

943   consequently the formation of low-molecular weight aldehydes, declines (ox)PL digestibility by

944   pancreatic PLA_2. Moreover, it seems that this enzyme is responsible not only for direct PL digestion,

945   but also may modulate digestion of TAGs catalyzed by pancreatic lipase-colipase complex

946   (Borgström, 1980). The role of PLA_2 in neutral lipid digestion is to facilitate the access of lipase to

947   TAGs present in the core of lipid droplets surrounded by dietary and bile PLs. The initiation of PL

948   hydrolysis by PLA_2 results in binding of lipase to their substrates and rapid hydrolysis of TAGs

949   (Borgström, 1980). Taking the above into account, it can be hypothesized that PLA_2 activity decline in

950   the presence of oxidized (phospho)lipids is a physiological protective mechanism against too rapid

951   release of oxidized FAs, which similarly to their native counterparts may be effective absorbed by IECs

952   (Penumetcha, Khan, & Parthasarathy, 2000). Otherwise, in the cells exposed to relatively high

953   concentration of oxidized lipid hydrolysis products, the cellular redox homeostasis could become

954   disturbed and IEC death induced (T. Wang, Gotoh, Jennings, & Rhoads, 2000).

955   In order to examine this hypothesis, we evaluated the biological effect of PL oxidation and hydrolysis

956   towards HT29 cells serving as a model of IECs. However, it should be reminded the cell line used in

957   this study is characterized by cancerous origin. Therefore, due to some changes in nutrient transport

958   and metabolism as well as redox status, the tested compounds can affect the cells differentially

959   compared to healthy intestinal cells. Nevertheless, the aim of our research was to understand the

960   general mechanism of toxicity of oxidized PLs and products and their hydrolysis in the presence of

961   BSs, therefore we found this model to be appropriate. Based on the data obtained using MTT test, it

962   was observed that hydrolysis and oxidation of PLs led to significant decrease of cell viability in a time-

963   and concentration-dependent manner, while oxidized hydrolyzed PLs were characterized by the

964   highest cytotoxic effect (Fig. 3, Table A3). Additionally, BSs alone were found to decline HT29 cell

965   viability, especially for prolonged exposure time, compared to control cells treated with the buffer only.

966   However, this effect was reversed by the simultaneous presence of native non-hydrolyzed PLs across

967   the range of concentrations used. This observation can be explained by the limited bioavailability of

968   BSs for cells due to promoting the formation of less cytotoxic PL/BS mixed micelles/vesicles, which

969   was also confirmed by previous studies using other intestinal epithelium cell line delivered form human

970   colorectal adenocarcinoma – Caco-2 (Tan et al., 2013). Most probably, such a protective effect also

971   occurs under physiological conditions, where BSs are released to duodenum in the bile form

972   containing PLs. Bile is composed of 95 % water and various inorganic and organic compounds. The

973   letter include *i.a.* bile acids (40 mM), PLs (7 mM), cholesterol (3 mM) (Macierzanka, Torcello-Gómez,

974   Jungnickel, & Maldonado-Valderrama, 2019).

975   In addition, comet assay results showed that cell exposure to BS mixture caused significant DNA

976   strand breaks (Fig. 4). The genotoxic mechanism of BSs is not yet fully understood. It has been

977   suggested that DNA damage can be caused by the increased production of ROS and RNS *via*

978   stimulatory effect of BSs on the activation of LOX, cyclooxygenase (COX) and NADPH oxidase

979   (Nguyen, Ung, Kim, & Jung, 2018; Rosignoli et al., 2008). Moreover, BSs due to their surfactant

980   properties can cause mitochondrial damage, leading to the release of ROS generated in the

981   mitochondrial electron transport chain (Nguyen et al., 2018). However, the BS-induced genotoxicity

982   was reversed in the presence of not only native non-hydrolyzed PLs, as observed in the case of

983   cytotoxic effect of BS, but also in cells treated with oxidized and hydrolysed samples. Moreover, higher

984   lipid concentration (250 vs. 125 µg/mL) led to statistically significant stronger protection against BS-

985   induced genotoxicity for all sample types. This observation indicates that cytotoxic effect caused by

986   prolonged cell exposure to higher concentrations of native hydrolyzed and oxidized, both non-

987   hydrolyzed and hydrolyzed PLs, was not related to DNA strand breaks, as determined using comet

988   assay. Most probably, for HT29 cells treated with these samples, an overlap of other toxic effects was

989   observed. For example, hydrolysis of both native and oxidized PLs significantly affected the cellular

990 accumulation of neutral lipids. The products of PL hydrolysis (LPLs and FAs), after intestinal

991 absorption, are re-esterified at the ER membrane (Küllenberg de Gaudry et al., 2012). However, the

992 prolonged cell exposure to high concentration of LPLs and FAs can lead to excessive of cellular PL

993 levels causing alterations in cellular lipid metabolism. The previous data showed that cell exposure to

994 exogenous LPCs or LPEs led to increased synthesis of cellular PCs. However, the cells compensated

995 this elevated PC level by their enzymatic degradation to glycerophosphocholine (GPC) and FA by

996 lysophospholipase (lysoPLA$_1$) activity (Baburina & Jackowski, 1999).

997 Additionally, taking into account the presence of FAs delivered from egg yolk PL hydrolysis in the

998 culture medium, cellular esterification of these FAs to TAGs would be necessary to limit their lipotoxic

999 effect (Lipke, Kubis-Kubiak, & Piwowar, 2022). This metabolic pathway most probably led to increased

1000 accumulation of TAGs in the cytosolic droplets within the cells exposed to hydrolyzed native and

1001 oxidized PLs. However, long-term cell exposure to high concentration of PL hydrolysis products could

1002 lead to the intensification of the lipotoxic effect, which was manifested as decreased cell viability.

1003 Importantly, under the lipotoxic conditions, the increased mitochondrial FA oxidation can occur in order

1004 to metabolize the cellular lipid excess. This can lead to disturbance of cellular redox homeostasis and

1005 increased lipid peroxidation accompanied by the formation of other toxic compounds such as

1006 electrophilic α,β-unsaturated 4-hydroxyalkenals, which are capable of covalent modification of cellular

1007 proteins or DNA. Such type of DNA damage however, may not be detected by comet assay used in

1008 this study. This method determines DNA strand fragmentation, but not necessarily the stable covalent

1009 modifications of nucleic acid bases by aldehydes.

1010 HT29 cell exposure to non-hydrolyzed oxidized PLs led to a significant decrease of their viability,

1011 especially for prolonged incubation times. On the one hand, absorption of (phospho)lipid oxidation

1012 products containing reactive functional groups, such as hydroperoxide or aldehyde, can led to

1013 modification of cellular structures such as proteins, membrane lipids and DNA, as well as may disturb

1014 the cellular redox homeostasis. The previous research using other cell line – Caco-2 – confirmed our

1015 observations and conclusions. The exposure of Caco-2 cells to not-hydrolyzed oxidized menhaden oil

016 lead to significant GSH/GSSG ratio, inducing cellular redox imbalance and initiation of apoptotic cell

017 death (T. Wang et al., 2000). Moreover, the literature data indicated that oxPLs can trigger numerous

018 signaling pathways leading also to cellular apoptosis as well as inflammation induction (Fruhwirth et

019 al., 2007). Interestingly, the biggest differences in the cell viability curves were observed between

38

1020   native hydrolyzed, oxidized non-hydrolyzed and oxidized hydrolyzed PLs for the cells exposed the

1021   shortest incubation time (6 h). This indicates that while comparing all, the release of oxidized FAs from

1022   the *sn*-2 position of PLs in a short time induced the highest cytotoxic effect among all tested samples.

1023   An *in vitro* studies using Caco-2 cell line indicated that hydroperoxy octadecadienoic acid (HPODE)

1024   and hydroxy octadecadienoic acid (HODE) were effectively absorbed by cells within the exposure time

1025   of 30 min. Additionally, the uptake of modified FAs was comparable to non-oxidized FAs such as

1026   linoleic or oleic (Penumetcha et al., 2000). In contrast, the absorption of these oxidized FAs was

1027   significantly (about 20 times) lower for smooth muscle cells (Penumetcha et al., 2000). One of the

1028   most common oxidized FA is 13-hydroperoxy octadecadienoic acid (13-HPODE). In addition to

1029   inducing oxidative stress and cellular death at higher concentrations (above 100 µM) and insufficient

1030   activity of GPx2 enzyme, an *in vitro* studies using Caco-2 model showed that subtoxic concentration of

1031   13-HPODE can induce pro-inflammatory gene expression and affect lipid and glucose metabolism,

1032   energy production and mitochondrial functions (Faizo, Narasimhulu, Forsman, Yooseph, &

1033   Parthasarathy, 2021; Keewan, Narasimhulu, Rohr, Hamid, & Parthasarathy, 2020).

1034   **5. Conclusions**

1035   Oxidation of dietary (phospho)lipids is associated not only with the deterioration of the quality and

1036   sensory properties of foodstuffs, but also may pose a serious threat to the health of consumers,

1037   especially leading to some gastrointestinal pathologies. Firstly, our results indicated that oxidation of

1038   PLs decreased their hydrolysis catalyzed by pancreatic PLA$_2$ in the presence of BS mixture. We

1039   suggested that low-molecular weight aldehydes such as hexanal or (*E*)-2-nonenal, which are formed

1040   as a result of lipid hydroperoxide breakdown by the cleavage of the C-C bond in UFA chains, can

1041   covalently modify the enzyme leading to inhibition of its activity. Our further research using HT29 cell

1042   line indicated that both hydrolysis and oxidation of PLs led to decrease of cell viability in a time- and

1043   concentration-dependent manner, while combination of both these factors resulted in the highest

1044   cytotoxic effect determined by MTT test. On the other hand, the BS-induced genotoxic effect was

1045   reversed in the presence PLs regardless of whether they were oxidized or hydrolyzed, while the

046   protective effect against the BS-induced cytotoxicity was observed for native non-hydrolyzed PLs, but

047   was not clearly visible for other samples. This can be related to an overlap of several toxic effects

048   including lipotoxicity or disturbance of cellular redox homeostasis. The obtained data have driven us to

049   a non-obvious conclusion that the inhibition of PLA$_2$ activity in the presence of oxidized

1050 (phospho)lipids, may be a kind of physiological protective mechanism against rapid release of oxidized

1051 FAs that are characterized by cytotoxic effect towards IECs.

6. Limitation of the study

1053 It should be noted that the presented work was aimed at a preliminary assessment of the influence of

1054 oxidative modification of dietary (phospho)lipids on their digestion and biological effects towards

1055 intestinal epithelium. Therefore, to understand the fundamental mechanisms or their action, the

1056 proposed models did not fully reflect the physiological conditions (e.g., only the intestinal phase of

1057 digestion was considered; only one of pancreatic lipolytic enzymes was used; there were no other

1058 nutrients such as protein included). However, despite simplified experimental design, it was possible

1059 to observe the important differences between native and oxidized egg yolk PL fractions on PL

1060 hydrolysis as well as cell physiology and pathophysiology. Nevertheless, further work in this area is

1061 needed for a deeper understanding of mechanisms occurring under the physiological conditions.

CRediT authorship contribution statement

1063 **Karol Parchem:** Conceptualization, Data Curation, Formal analysis, Funding Acquisition,

1064 Investigation, Methodology, Project Administration, Validation, Visualization, Writing –

1065 original draft, Writing – review & editing. **Monika Baranowska:** Investigation, Methodology,

1066 Validation. **Anna Kościelak:** Investigation. **Ilona Kłosowska-Chomiczewska:** Investigation,

1067 Methodology, Validation. **Maria Rosário Domingues:** Funding Acquisition, Supervision,

1068 Writing – review & editing. **Adam Macierzanka:** Supervision, Writing – review & editing.

1069 **Agnieszka Bartoszek:** Conceptualization, Formal analysis, Funding Acquisition, Resources,

1070 Supervision, Visualization, Writing – original draft, Writing – review & editing.

Declaration of Competing Interest

1072 The authors declare that they have no known competing financial interests or personal

1073 relationships that could have appeared to influence the work reported in this paper.

40

1079   research units LAQV-REQUIMTE [grant number UIDB/50006/2020] and CESAM [grant number

1080   UIDP/50017/2020 + UIDB/50017/2020 + LA/P/0094/2020].

1081   **Appendix A. Supplementary data**

1082   Supplementary data to this article can be found online.

1083   **References**

1084   Andrews, J. S., Griffith, W. H., Mead, J. F., & Stein, R. A. (1960). Toxicity of air-oxidized soybean oil.
1085   *The Journal of Nutrition*, *70*(2), 199–210.
1086   Awada, M., Soulage, C. O., Meynier, A., Debard, C., Plaisancié, P., Benoit, B., … Michalski, M. C.
1087   (2012). Dietary oxidized n-3 PUFA induce oxidative stress and inflammation: Role of intestinal
1088   absorption of 4-HHE and reactivity in intestinal cells. *Journal of Lipid Research*, *53*(10), 2069–
1089   2080. https://doi.org/10.1194/jlr.M026179
1090   Baba, N., Mikami, Y., Shigeta, Y., Nakajima, S., & Matsuo, M. (1993). Hydrolysis of
1091   glycerophosphocholine hydroperoxide by phospholipase A2. *Bioscience, Biotechnology, and*
1092   *Biochemistry*, *51*(12), 2200–2201. https://doi.org/10.1271/bbb.57.2200
1093   Baburina, I., & Jackowski, S. (1999). Cellular responses to excess phospholipid. *Journal of Biological*
1094   *Chemistry*, *274*(14), 9400–9408. https://doi.org/10.1074/jbc.274.14.9400
1095   Baranowska, M., Koziara, Z., Suliborska, K., Chrzanowski, W., Wormstone, M., Namieśnik, J., &
1096   Bartoszek, A. (2021). Interactions between polyphenolic antioxidants quercetin and naringenin
1097   dictate the distinctive redox-related chemical and biological behaviour of their mixtures. *Scientific*
1098   *Reports*, *11*(1), 1–18. https://doi.org/10.1038/s41598-021-89314-0
1099   Baranowska, M., Suliborska, K., Chrzanowski, W., Kusznierewicz, B., Namie, J., & Bartoszek, A.
1100   (2018). The relationship between standard reduction potentials of catechins and biological
1101   activities involved in redox control. *Redox Biology*, *17*, 355–366.
1102   https://doi.org/10.1016/j.redox.2018.05.005
1103   Baranowska, M., Suliborska, K., Todorovic, V., Kusznierewicz, B., Chrzanowski, W., Sobajic, S., &
1104   Bartoszek, A. (2020). Interactions between bioactive components determine antioxidant,
1105   cytotoxic and nutrigenomic activity of cocoa powder extract. *Free Radical Biology and Medicine*,
1106   *154*, 48–61. https://doi.org/10.1016/j.freeradbiomed.2020.04.022
1107   Bashllari, R., Molonia, M. S., Muscarà, C., Speciale, A., Wilde, P. J., Saija, A., & Cimino, F. (2020).
1108   Cyanidin-3-O-glucoside protects intestinal epithelial cells from palmitate-induced lipotoxicity.
1109   *Archives of Physiology and Biochemistry*, 1–8. https://doi.org/10.1080/13813455.2020.1828480
1110   Beilstein, F., Carrière, V., Leturque, A., & Demignot, S. (2016). Characteristics and functions of lipid
1111   droplets and associated proteins in enterocytes. *Experimental Cell Research*, *340*(2), 172–179.
1112   https://doi.org/10.1016/j.yexcr.2015.09.018
1113   Beisson, F., Tiss, A., Rivière, C., & Verger, R. (2000). Methods for lipase detection and assay: A
1114   critical review. *European Journal of Lipid Science and Technology*, *102*(2), 133–153.
1115   https://doi.org/10.1002/(sici)1438-9312(200002)102:2<133::aid-ejlt133>3.0.co;2-x
1116   Birru, W. A., Warren, D. B., Ibrahim, A., Williams, H. D., Benameur, H., Porter, C. J. H., … Pouton, C.
1117   W. (2014). Digestion of phospholipids after secretion of bile into the duodenum changes the
1118   phase behavior of bile components. *Molecular Pharmaceutics*, *11*(8), 2825–2834.
1119   https://doi.org/10.1021/mp500193g
1120   Blesso, C. N. (2015). Egg phospholipids and cardiovascular health. *Nutrients*, *7*(4), 2731–2747.
1121   https://doi.org/10.3390/nu7042731
1122   Borgström, B. (1980). Importance of phospholipids, pancreatic phospholipase A2, and fatty acid for
1123   the digestion of dietary fat in vitro experiments enzymes. *Gastroenterology*, *78*, 954–962.
1124   Brash, A. R. (1999). Lipoxygenases: Occurrence, functions, catalysis, and acquisition of substrate.
125   *The Journal of Biological Chemistry*, *274*(34), 23679–23683.
126   Butler O'Connor, E. S., Mazerik, J. N., Cruff, J. P., Sherwani, S. I., Weis, B. K., Marsh, C. B., …
127   Parinandi, N. L. (2010). Lipoxygenase-catalyzed phospholipid peroxidation: Preparation,
128   purification, and characterization of phosphatidylinositol peroxides. In R. M. Uppu, S. N. Murthy,
129   W. A. Pryor, & N. L. Parinandi (Eds.), *Free Radicals and Antioxidant Protocols. Methods in*
130   *Molecular Biology (Methods and Protocols)* (2nd ed., pp. 387–401). Humana Press.
131   https://doi.org/10.1007/978-1-60327-029-8
132   Catalá, A. (2012). Lipid peroxidation modifies the picture of membranes from the "Fluid Mosaic Model"
133   to the "Lipid Whisker Model." *Biochimie*, *94*(1), 101–109.

https://doi.org/10.1016/j.biochi.2011.09.025

Catalá, A. (2015). Lipid peroxidation modifies the assembly of biological membranes "The Lipid Whisker Model." *Frontiers in Physiology*, *5*(520), 1–4. https://doi.org/10.3389/fphys.2014.00520

Catalá, A., & Díaz, M. (2016). Editorial: Impact of lipid peroxidation on the physiology and pathophysiology of cell membranes. *Frontiers in Physiology*, *7*(423), 1–3. https://doi.org/10.3389/fphys.2016.00423

Catalán, V., Frühbeck, G., & Gómez-Ambrosi, J. (2018). Inflammatory and oxidative stress markers in skeletal muscle of obese subjects. In A. Marti del Moral & C. M. Aguilera (Eds.), *Obesity* (pp. 163–189). Academic Press. https://doi.org/10.1016/B978-0-12-812504-5.00008-8

Chen, D. W., Balagiannis, D. P., & Parker, J. K. (2019). Use of egg yolk phospholipids to generate chicken meat odorants. *Food Chemistry*, *286*, 71–77. https://doi.org/10.1016/j.foodchem.2019.01.184

Cui, L., & Decker, E. A. (2016). Phospholipids in foods: Prooxidants or antioxidants? *Journal of the Science of Food and Agriculture*, *96*(1), 18–31. https://doi.org/10.1002/jsfa.7320

Dennis, E. A., Cao, J., Hsu, Y.-H., Magrioti, V., & Kokotos, G. (2011). Phospholipase A2 enzymes: Physical structure, biological function, disease implication, chemical inhibition, and therapeutic intervention. *Chemical Reviewseviews*, *111*(10), 6130–6185. https://doi.org/10.1021/cr200085w.Phospholipase

Dittmer, J. C., & Lester, R. L. (1964). A simple, specific spray for the detection of phospholipids on thin-layer chromatograms. *Journal of Lipid Research*, *5*(1), 126–127.

Domínguez, R., Pateiro, M., Gagaoua, M., Barba, F. J., Zhang, W., & Lorenzo, J. M. (2019). A comprehensive review on lipid oxidation in meat and meat products. *Antioxidants*, *8*(10), 1–31. https://doi.org/10.3390/antiox8100429

Faizo, N., Narasimhulu, C. A., Forsman, A., Yooseph, S., & Parthasarathy, S. (2021). Peroxidized linoleic acid, 13-HPODE, alters gene expression profile in intestinal epithelial cells. *Foods*, *10*(2), 1–23. https://doi.org/10.3390/foods10020314

Fedi, A., Vitale, C., Ponschin, G., Ayehunie, S., Fato, M., & Scaglione, S. (2021). In vitro models replicating the human intestinal epithelium for absorption and metabolism studies: A systematic review. *Journal of Controlled Release*, *335*, 247–268. https://doi.org/10.1016/j.jconrel.2021.05.028

Fenaille, F., Mottier, P., Turesky, R. J., Ali, S., & Guy, P. A. (2001). Comparison of analytical techniques to quantify malondialdehyde in milk powders. *Journal of Chromatography A*, *921*(2), 237–245. https://doi.org/10.1016/S0021-9673(01)00883-4

Fruehwirth, S., Zehentner, S., Salim, M., Sterneder, S., Tiroch, J., Lieder, B., … Pignitter, M. (2020). In vitro digestion of grape seed oil inhibits phospholipid-regulating effects of oxidized lipids. *Biomolecules*, *10*(708), 1–20. https://doi.org/10.3390/biom10050708

Fruhwirth, G. O., Loidl, A., & Hermetter, A. (2007). Oxidized phospholipids: From molecular properties to disease. *Biochimica et Biophysica Acta - Molecular Basis of Disease*, *1772*(7), 718–736. https://doi.org/10.1016/j.bbadis.2007.04.009

Gilbraith, W. E., Carter, J. C., Adams, K. L., Booksh, K. S., & Ottaway, J. M. (2021). Improving prediction of peroxide value of edible oils using regularized regression models. *Molecules*, *26*(23), 1–20. https://doi.org/10.3390/molecules26237281

Girón-Calle, J., Schmid, P. C., & Schmid, H. H. O. (1997). Effects of oxidative stress on glycerolipid acyl turnover in rat hepatocytes. *Lipids*, *32*(9), 917–923. https://doi.org/10.1007/s11745-997-0118-9

Gładkowski, W., Chojnacka, A., Kiełbowicz, G., Trziszka, T., & Wawrzeńczyk, C. (2012). Isolation of pure phospholipid fraction from egg yolk. *Journal of the American Oil Chemists' Society*, *89*(1), 179–182. https://doi.org/10.1007/s11746-011-1893-x

Gotoh, N., Watanabe, H., Osato, R., Inagaki, K., Iwasawa, A., & Wada, S. (2006). Novel approach on the risk assessment of oxidized fats and oils for perspectives of food safety and quality. I. Oxidized fats and oils induces neurotoxicity relating pica behavior and hypoactivity. *Food and Chemical Toxicology*, *44*(4), 493–498. https://doi.org/10.1016/j.fct.2005.08.023

Grootveld, M., Percival, B. C., Leenders, J., & Wilson, P. B. (2020). Potential adverse public health effects afforded by the ingestion of dietary lipid oxidation product toxins: Significance of fried food sources. *Nutrients*, *12*(974), 1–49. https://doi.org/10.3390/nu12040974

Gulhane, M., Murray, L., Lourie, R., Tong, H., Sheng, Y. H., Wang, R., … Hasnain, S. Z. (2016). High fat diets induce colonic epithelial cell stress and inflammation that is reversed by IL-22. *Scientific Reports*, *6*, 1–17. https://doi.org/10.1038/srep28990

Gundermann, K. J., Gundermann, S., Drozdzik, M., & Mohan Prasad, V. G. (2016). Essential phospholipids in fatty liver: A scientific update. *Clinical and Experimental Gastroenterology*, *9*,

105–117. https://doi.org/10.2147/CEG.S96362

Gupta, A., Eral, H. B., Hatton, T. A., & Doyle, P. S. (2016). Nanoemulsions: Formation, properties and applications. *Soft Matter*, *12*(11), 2826–2841. https://doi.org/10.1039/c5sm02958a

Guyon, C., Meynier, A., & de Lamballerie, M. (2016). Protein and lipid oxidation in meat: A review with emphasis on high-pressure treatments. *Trends in Food Science and Technology*, *50*, 131–143. https://doi.org/10.1016/j.tifs.2016.01.026

Henning, R. J., Johnson, G. T., Coyle, J. P., & Harbison, R. D. (2017). Acrolein can cause cardiovascular disease: A review. *Cardiovascular Toxicology*, *17*(3), 227–236. https://doi.org/10.1007/s12012-016-9396-5

Igene, J. O., Pearson, A. M., Dugan, L. R., & Price, J. F. (1980). Role of triglycerides and phospholipids on development of rancidity in model meat systems during frozen storage. *Food Chemistry*, *5*(4), 263–276. https://doi.org/10.1016/0308-8146(80)90048-5

Jackson, V., & Penumetcha, M. (2019). Dietary oxidised lipids, health consequences and novel food technologies that thwart food lipid oxidation: an update. *International Journal of Food Science and Technology*, *54*(6), 1981–1988. https://doi.org/10.1111/ijfs.14058

Jacobsen, C., Paiva-Martins, F., Schwarz, K., & Bochkov, V. (2019). Lipid oxidation and antioxidants in food and nutrition. *European Journal of Lipid Science and Technology*, *121*(9), 1–1. https://doi.org/10.1002/ejlt.201900298

Jiang, K., Huang, C., Liu, F., Zheng, J., Ou, J., Zhao, D., & Ou, S. (2022). Origin and fate of acrolein in foods. *Foods*, *11*(13), 1–24. https://doi.org/10.3390/foods11131976

Jiménez-Rojo, N., Viguera, A. R., Collado, M. I., Sims, K. H., Constance, C., Hill, K., … Alonso, A. (2014). Sphingosine induces the aggregation of imine-containing peroxidized vesicles. *Biochimica et Biophysica Acta - Biomembranes*, *1838*(8), 2071–2077. https://doi.org/10.1016/j.bbamem.2014.04.028

Jittrepotch, N., Ushio, H., & Ohshima, T. (2006). Oxidative stabilities of triacylglycerol and phospholipid fractions of cooked Japanese sardine meat during low temperature storage. *Food Chemistry*, *99*(2), 360–367. https://doi.org/10.1016/j.foodchem.2005.08.002

Kambayashi, Y., Yamamoto, Y., & Nakan, M. (1998). Preferential hydrolysis of oxidized phosphatidylcholine in cholesterol-containing phosphatidylcholine liposome by phospholipase A2. *Biochemical and Biophysical Research Communications*, *245*(3), 705–708.

Kanner, J. (2007). Dietary advanced lipid oxidation endproducts are risk factors to human health. *Molecular Nutrition & Food Research*, *51*(9), 1094–1101. https://doi.org/10.1002/mnfr.200600303

Keewan, E., Narasimhulu, C. A., Rohr, M., Hamid, S., & Parthasarathy, S. (2020). Are fried foods unhealthy? The dietary peroxidized fatty acid, 13-HPODE, induces intestinal inflammation in vitro and in vivo. *Antioxidants*, *9*(10), 1–17. https://doi.org/10.3390/antiox9100926

Kölbel, K., Weininger, U., Ihling, C., Mrestani-Klaus, C., & Ulbrich-Hofmann, R. (2015). Native state dynamics affects the folding transition of porcine pancreatic phospholipase A2. *Biophysical Chemistry*, *206*, 12–21. https://doi.org/10.1016/j.bpc.2015.06.007

Krishna, G., & Gopalakrishnan, G. (2016). Alternative in vitro models for safety and toxicity evaluation of nutraceuticals. In R. C. Gupta (Ed.), *Nutraceuticals* (pp. 355–386). Academic Press. https://doi.org/10.1016/B978-0-12-802147-7.00027-9

Küllenberg de Gaudry, D., Taylor, L. a, Schneider, M., & Massing, U. (2012). Health effects of dietary phospholipids. *Lipids in Health and Disease*, *11*(1), 1–16. https://doi.org/10.1186/1476-511X-11-3

Kupper, S., Kłosowska-Chomiczewska, I., & Szumała, P. (2017). Collagen and hyaluronic acid hydrogel in water-in-oil microemulsion delivery systems. *Carbohydrate Polymers*, *175*, 347–354. https://doi.org/10.1016/j.carbpol.2017.08.010

Lian, C. Y., Zhai, Z. Z., Li, Z. F., & Wang, L. (2020). High fat diet-triggered non-alcoholic fatty liver disease: A review of proposed mechanisms. *Chemico-Biological Interactions*, *330*, 1–15. https://doi.org/10.1016/j.cbi.2020.109199

Lipke, K., Kubis-Kubiak, A., & Piwowar, A. (2022). Molecular mechanism of lipotoxicity as an interesting aspect in the development of pathological states - Current view of knowledge. *Cells*, *11*(844), 1–34. https://doi.org/10.3390/cells11050844

Lísa, M., Cífková, E., & Holčapek, M. (2011). Lipidomic profiling of biological tissues using off-line two-dimensional high-performance liquid chromatography-mass spectrometry. *Journal of Chromatography A*, *1218*(31), 5146–5156. https://doi.org/10.1016/j.chroma.2011.05.081

Listenberger, L. L., & Brown, D. A. (2007). Fluorescent detection of lipid droplets and associated proteins. *Current Protocols in Cell Biology*, *35*(1), 24.2.1-24.2.11.

Litvinko, N. M., Skorostetskaya, L. A., & Gerlovsky, D. O. (2018). The interaction of phospholipase A2 with oxidized phospholipids at the lipid-water surface with different structural organization.

Chemistry and Physics of Lipids, *211*, 44–51. https://doi.org/10.1016/j.chemphyslip.2017.10.010

Macierzanka, A., Torcello-Gómez, A., Jungnickel, C., & Maldonado-Valderrama, J. (2019). Bile salts in digestion and transport of lipids. *Advances in Colloid and Interface Science*, *274*, 1–17. https://doi.org/10.1016/j.cis.2019.102045

Maldonado-Valderrama, J., Wilde, P., Macierzanka, A., & MacKie, A. (2011). The role of bile salts in digestion. *Advances in Colloid and Interface Science*, *165*(1), 36–46. https://doi.org/10.1016/j.cis.2010.12.002

Martin-Rubio, A. S., Sopelana, P., Ibargoitia, M. L., & Guillén, M. D. (2021). 1H NMR study of the in vitro digestion of highly oxidized soybean oil and the effect of the presence of ovalbumin. *Foods*, *10*(7), 1–26. https://doi.org/10.3390/foods10071573

Martínez-Maqueda, D., Miralles, B., & Recio, I. (2015). HT29 cell line. In K. Verhoeckx, P. Cotter, I. López-Expósito, C. Kleiveland, T. Lea, A. Mackie, … H. Wichers (Eds.), *The Impact of Food Bioactives on Health: In Vitro and Ex Vivo Models* (1st ed., pp. 113–124). Springer Cham. https://doi.org/10.1007/978-3-319-16104-4

Meca, A. D., Turcu-Stiolica, A., Stanciulescu, E. C., Andrei, A. M., Nitu, F. M., Banita, I. M., … Pisoschi, C. G. (2021). Variations of serum oxidative stress biomarkers under first-line antituberculosis treatment: A pilot study. *Journal of Personalized Medicine*, *11*(2), 1–10. https://doi.org/10.3390/jpm11020112

Meyuhas, D., Bor, A., Pinchuk, I., Kaplun, A., Talmon, Y., Kozlov, M. M., & Lichtenberg, D. (1997). Effect of ionic strength on the self-assembly in mixtures of phosphatidylcholine and sodium cholate. *Journal of Colloid and Interface Science*, *188*(2), 351–362.

Montgomery, M. K., De Nardo, W., & Watt, M. J. (2019). Impact of lipotoxicity on tissue "cross talk" and metabolic regulation. *Physiology*, *34*(2), 134–149. https://doi.org/10.1152/physiol.00037.2018

Nguyen, T. T., Ung, T. T., Kim, N. H., & Jung, Y. Do. (2018). Role of bile acids in colonic carcinogenesis. *World Journal of Clinical Cases*, *6*(13), 577–588. https://doi.org/10.1007/BF01734247

Nicolson, G. L., & Ash, M. E. (2014). Lipid Replacement Therapy: A natural medicine approach to replacing damaged lipids in cellular membranes and organelles and restoring function. *Biochimica et Biophysica Acta - Biomembranes*, *1838*(6), 1657–1679. https://doi.org/10.1016/j.bbamem.2013.11.010

Nieva-Echevarría, B., Goicoechea, E., & Guillén, M. D. (2018). Food lipid oxidation under gastrointestinal digestion conditions: A review. *Critical Reviews in Food Science and Nutrition*, *60*(3), 1–18. https://doi.org/10.1080/10408398.2018.1538931

Palusinska-Szysz, M., Kania, M., Turska-Szewczuk, A., & Danikiewicz, W. (2014). Identification of unusual phospholipid fatty acyl compositions of Acanthamoeba castellanii. *PloS One*, *9*(7), e101243. https://doi.org/10.1371/journal.pone.0101243

Pamplona, R. (2008). Membrane phospholipids, lipoxidative damage and molecular integrity: A causal role in aging and longevity. *Biochimica et Biophysica Acta - Bioenergetics*, *1777*(10), 1249–1262. https://doi.org/10.1016/j.bbabio.2008.07.003

Parchem, K., Kusznierewicz, B., Chmiel, T., Maciołek, P., & Bartoszek, A. (2019). Profiling and qualitative assessment of enzymatically and thermally oxidized egg yolk phospholipids using a two-step HPLC protocol. *Journal of the American Oil Chemists' Society*, *96*(6), 693–706.

Parchem, K., Sasson, S., Ferreri, C., & Bartoszek, A. (2019). Qualitative analysis of phospholipids and their oxidised derivatives–used techniques and examples of their applications related to lipidomic research and food analysis. *Free Radical Research*, *53*(sup1), 1068–1100. https://doi.org/10.1080/10715762.2019.1657573

Penumetcha, M., Khan, N., & Parthasarathy, S. (2000). Dietary oxidized fatty acids: an atherogenic risk? *Journal of Lipid Research*, *41*(9), 1473–1480.

Riethorst, D., Baatsen, P., Remijn, C., Mitra, A., Tack, J., Brouwers, J., & Augustijns, P. (2016). An in-depth view into human intestinal fluid colloids: Intersubject variability in relation to composition. *Molecular Pharmaceutics*, *13*, 3484–3493. https://doi.org/10.1021/acs.molpharmaceut.6b00496

Rosignoli, P., Fabiani, R., De Bartolomeo, A., Fuccelli, R., Pelli, M. A., & Morozzi, G. (2008). Genotoxic effect of bile acids on human normal and tumour colon cells and protection by dietary antioxidants and butyrate. *European Journal of Nutrition*, *47*(6), 301–309. https://doi.org/10.1007/s00394-008-0725-8

Sasson, S. (2017). Nutrient overload, lipid peroxidation and pancreatic beta cell function. *Free Radical Biology and Medicine*, *111*, 102–109. https://doi.org/10.1016/j.freeradbiomed.2016.09.003

Tan, Y., Qi, J., Lu, Y., Hu, F., Yin, Z., & Wu, W. (2013). Lecithin in mixed micelles attenuates the cytotoxicity of bile salts in Caco-2 cells. *Toxicology in Vitro*, *27*, 714–720.

1314   https://doi.org/10.1016/j.tiv.2012.11.018
1315   Tsunada, S., Iwakiri, R., Noda, T., Fujimoto, K., Fuseler, J., Rhoads, C. A., & Aw, T. Y. (2003).
1316   Chronic exposure to subtoxic levels of peroxidized lipids suppresses mucosal cell turnover in rat
1317   small intestine and reversal by glutathione. *Digestive Diseases and Sciences*, *48*(1), 210–222.
1318   https://doi.org/10.1023/A:1021775524062
1319   Van Rijn, J. M., Van Hoesel, M., De Heus, C., Van Vugt, A. H. M., Klumperman, J., Nieuwenhuis, E. E.
1320   S., … Middendorp, S. (2019). DGAT2 partially compensates for lipid-induced ER stress in human
1321   DGAT1-deficient intestinal stem cells. *Journal of Lipid Research*, *60*(10), 1787–1800.
1322   https://doi.org/10.1194/jlr.M094201
1323   Vieira, S. A., Zhang, G., & Decker, E. A. (2017). Biological implications of lipid oxidation products.
1324   *JAOCS, Journal of the American Oil Chemists' Society*, *94*(3), 339–351.
1325   https://doi.org/10.1007/s11746-017-2958-2
1326   Wang, T., Gotoh, Y., Jennings, M. H. O., & Rhoads, C. A. N. N. (2000). Lipid hydroperoxide-induced
1327   apoptosis in human colonic CaCo-2 cells is associated with an early loss of cellular redox
1328   balance. *The FASEB Journal*, *14*(11), 1567–1576.
1329   Wang, T. Y., Libardo, M. D. J., Angeles-Boza, A. M., & Pellois, J. P. (2017). Membrane oxidation in
1330   cell delivery and cell killing applications. *ACS Chemical Biology*, *12*(5), 1170–1182.
1331   https://doi.org/10.1021/acschembio.7b00237
1332   Wąsowicz, E., Gramza, A., Hęś, M., Jeleń, H. H., Korczak, J., Małecka, M., … Zawirska-Wojtasiak, R.
1333   (2004). Oxidation of lipids in foods. *Polish Journal of Food and Nutrition Science*, *13*(54), 87–
1334   100.
1335   Zierenberg, O., & Grundy, S. M. (1982). Intestinal absorption of polyenephosphatidylcholine in man.
1336   *Journal of Lipid Research*, *23*(8), 1136–1142. https://doi.org/10.1016/s0022-2275(20)38050-0
1337
1338